Ridziková Alexandra

Supervisor: doc. Ing. Jan Cepila, Ph.D.
11.09.2023
FNSPE CTU

RESEARCH THESIS

Energy dependence of hadron structure within quantum chromodynamics

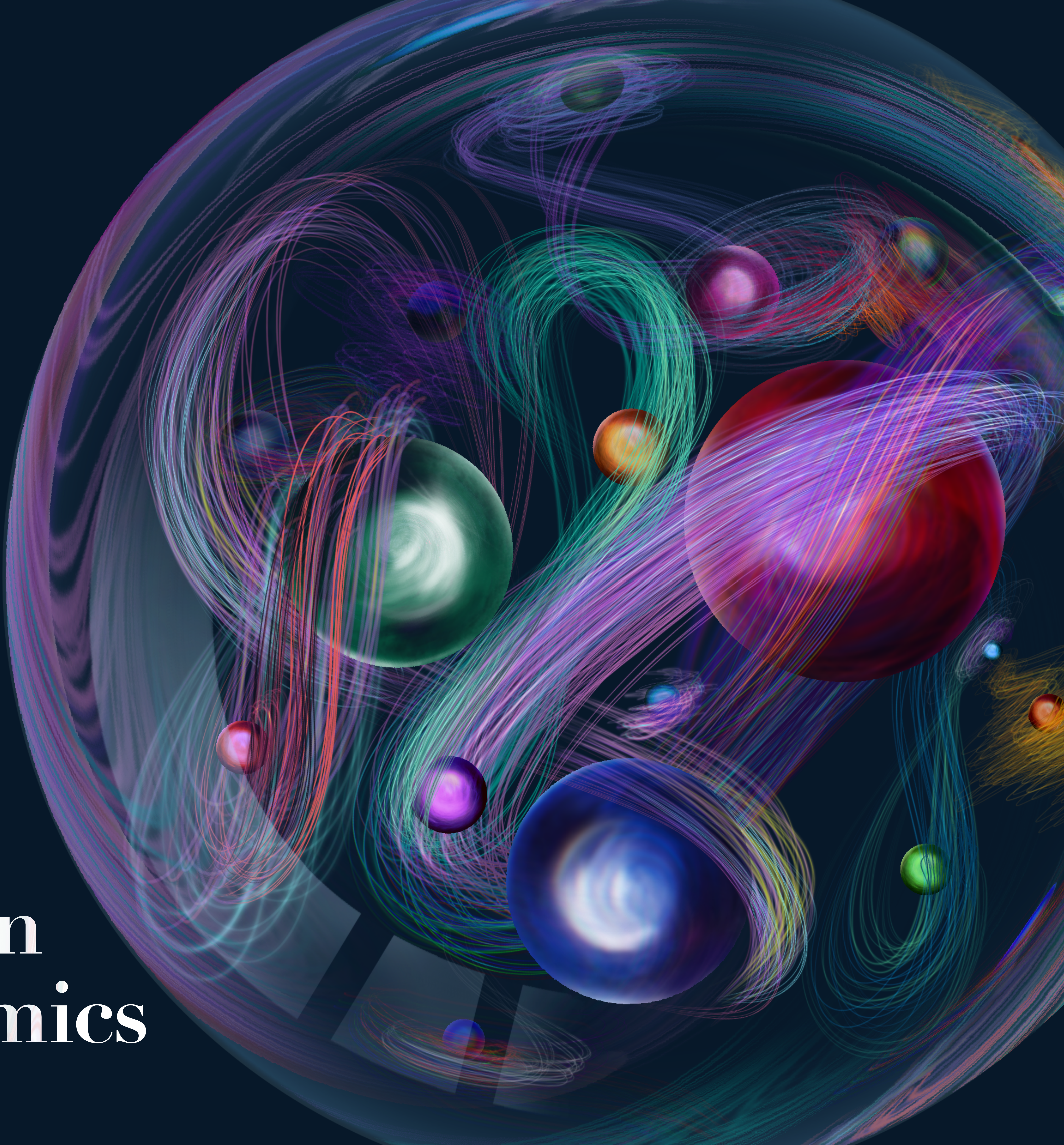

Motivation

- Evolution of parton densities
- At high momentum transfer and fixed x, an observation reveals the presence of a clusters of smaller partons. The vertical direction describes the evolution of the proton structure with increasing resolution scale Q^2 - DGLAP
- In the high-energy limit, which corresponds to small x, the density of partons increases significantly, and the partonic system is predominantly formed by gluons
  - Gluons may overlap and, eventually, interact
- ***Parton Saturation*** - dynamical balance between the gluon recombination and the radiation
  - Below saturation scale $Q_s^2(x)$ → dilute regime, linear gluon density evolution (BFKL)
  - Above $Q_s^2(x)$ → dense regime, non-linear gluon density evolution (JIMWLK, BK)

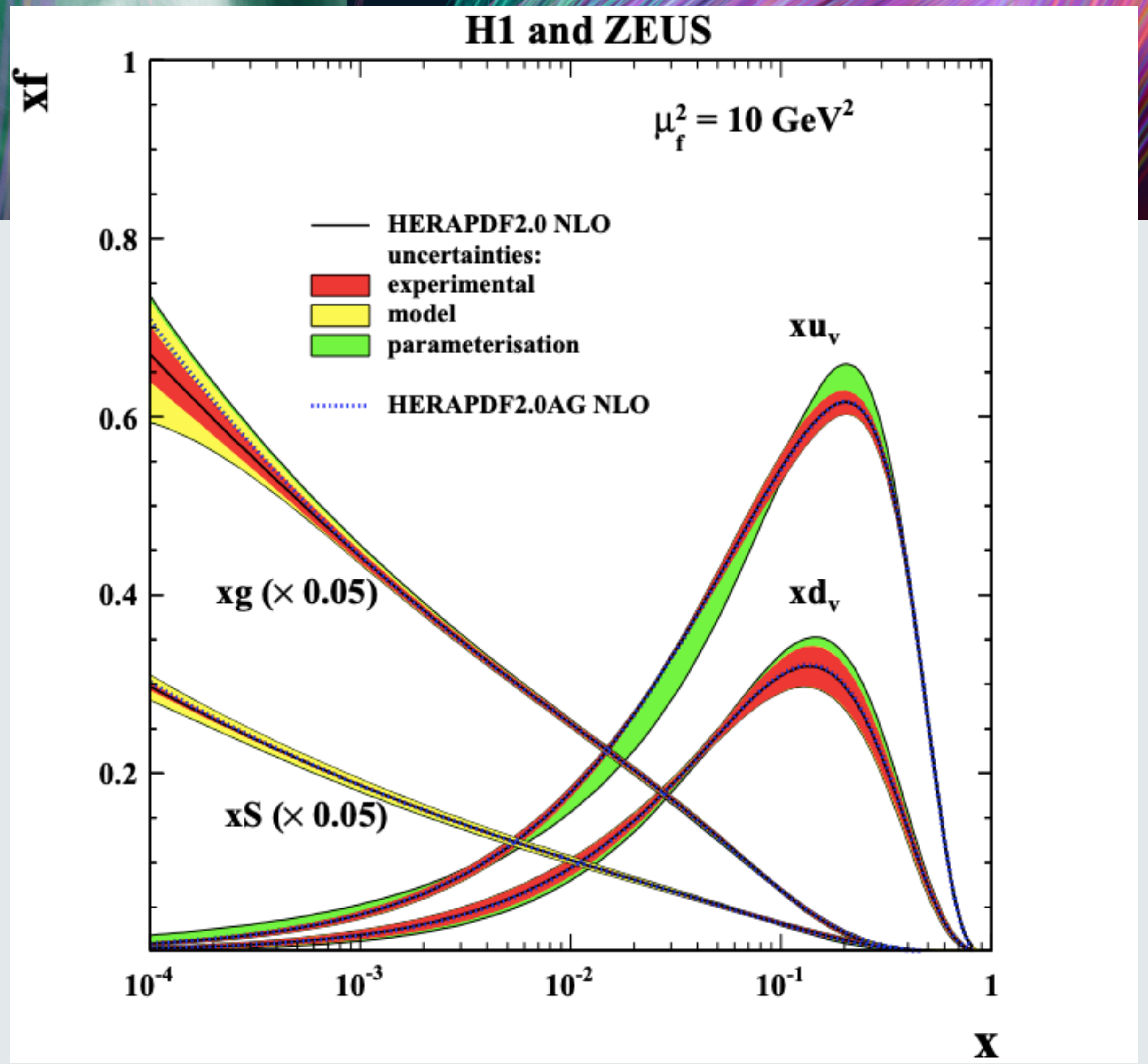

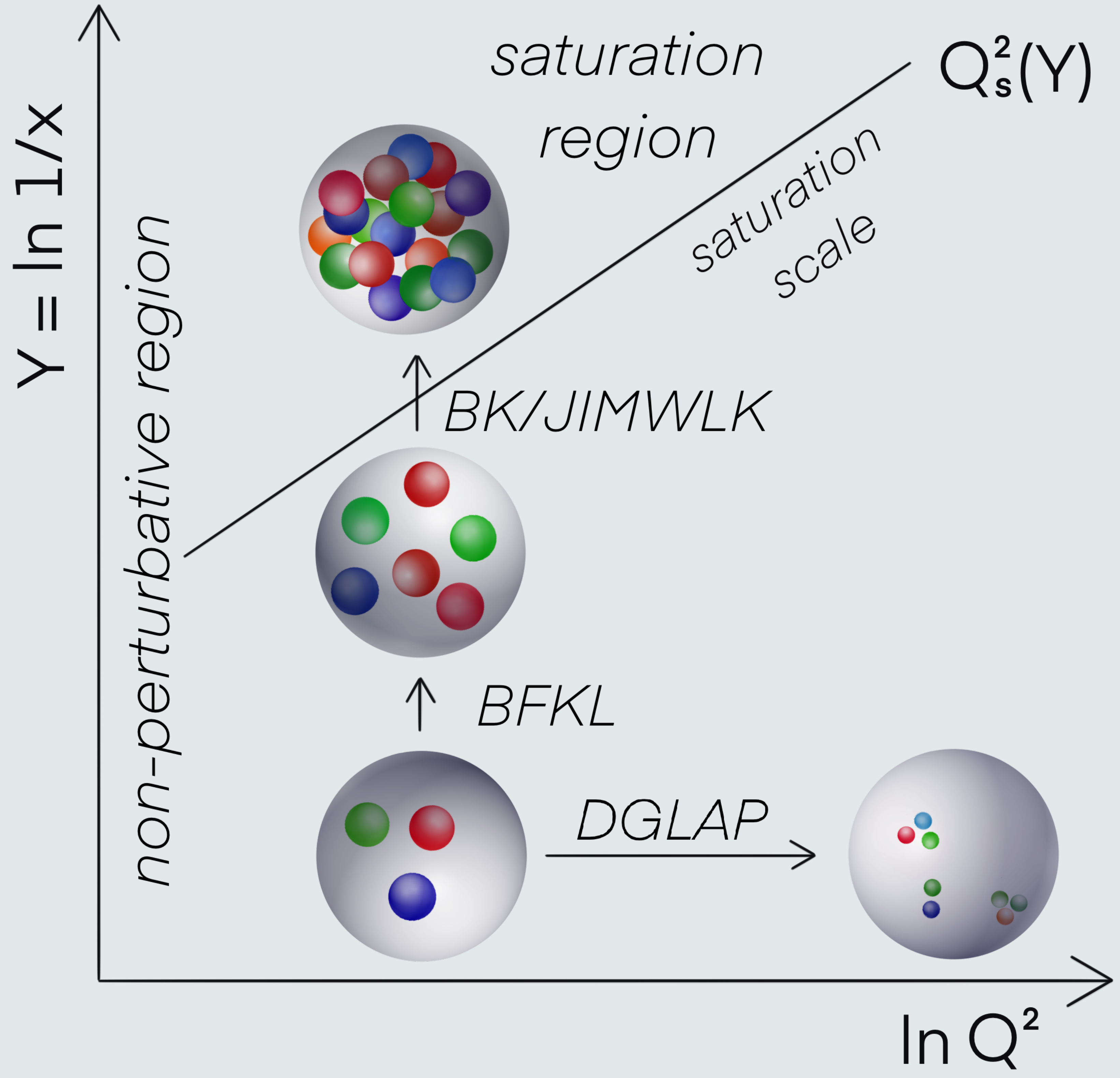

Vector meson production

- Process sensitive to the proton structure
- W is the center-of-mass energy of the photon-proton system
- $t = (p' - p)^2 = -\Delta^2$ square of the four-momentum transferred at the proton vertex
- Bjorken-x of the produced meson is $x = \dfrac{M_{VM}^2 + Q^2}{W^2 + Q^2}$
- M_{VM} is the mass of the vector meson and Q^2 is the virtuality of the incoming photon

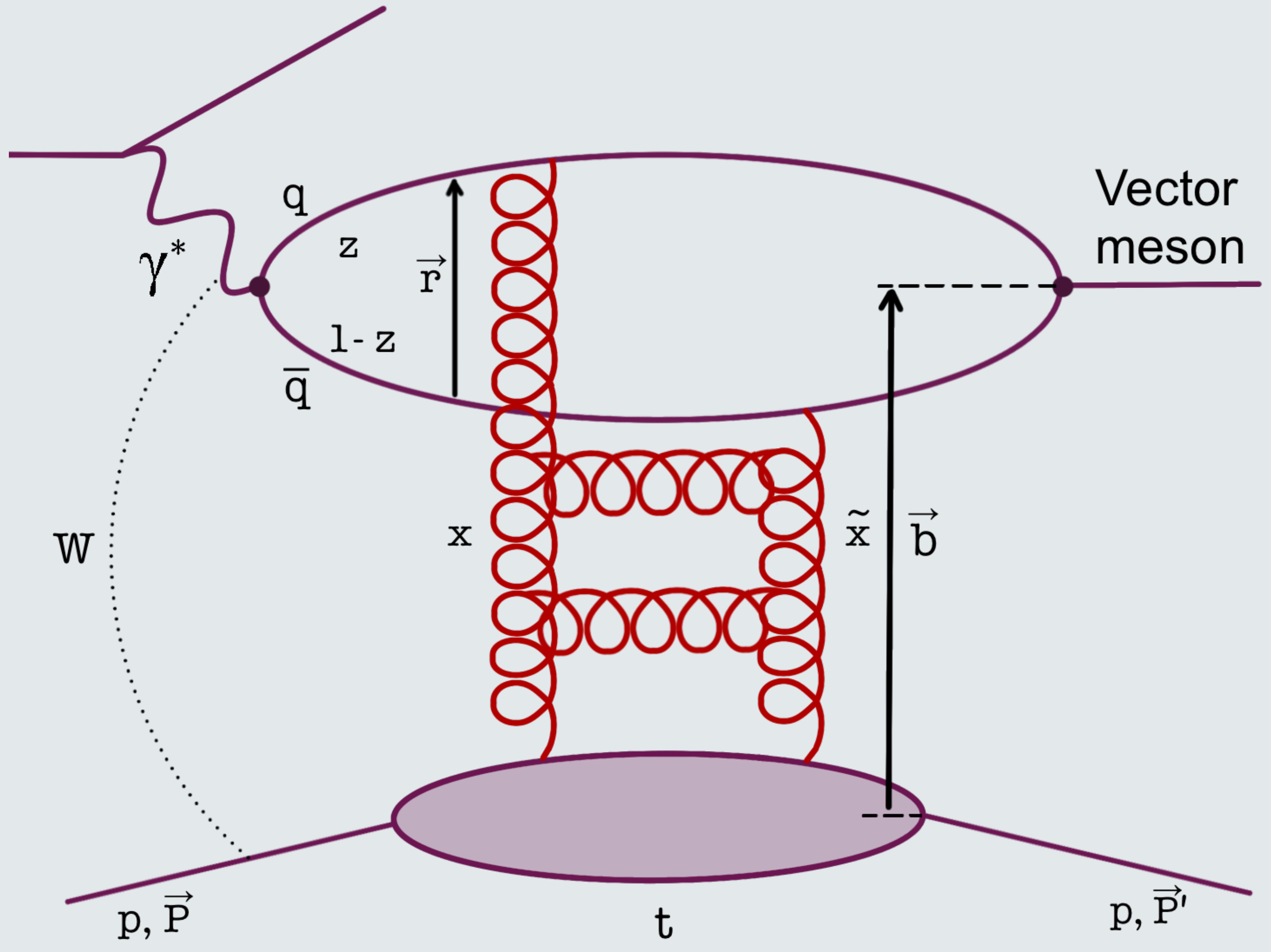

Exclusive - target proton remains intact

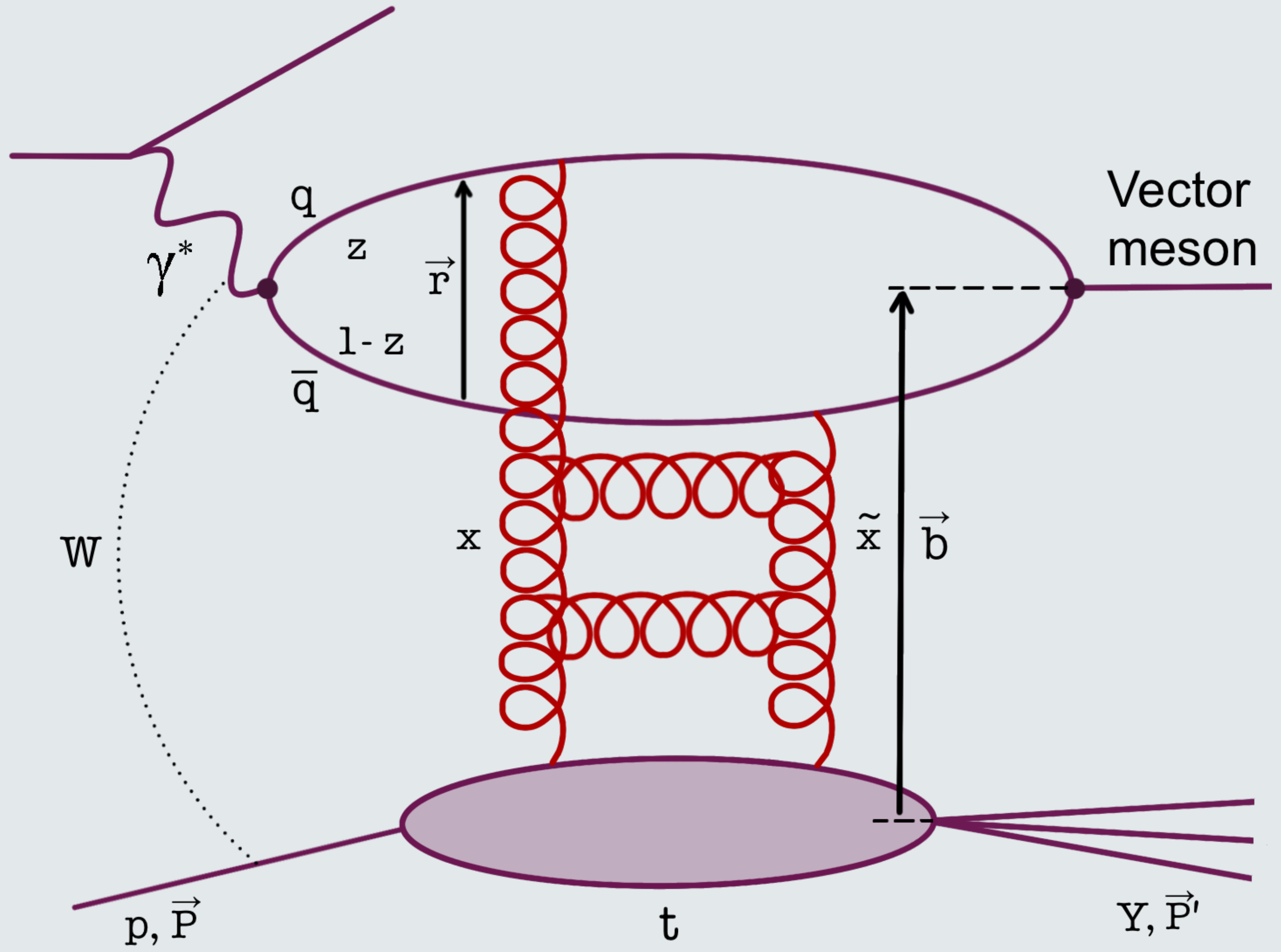

Dissociative - breakup of the target proton

Vector meson production

$$A_{T,L}^{\gamma^* p \to VMp}(x, Q^2, \Delta) = i \int \mathrm{d}\vec{r} \int_0^1 \frac{\mathrm{d}z}{4\pi} \int \mathrm{d}\vec{b} |\Psi_{VM}^* \Psi_{\gamma^*}|_{T,L} e^{-i[\vec{b}-(1-z)\vec{r}]\vec{\Delta}} \frac{\mathrm{d}\sigma_{q\bar{q}}}{\mathrm{d}\vec{b}}$$

- The scattering amplitude is given by the convolution of photon and vector meson wave functions $|\Psi_{VM}^* \Psi_{\gamma^*}|_{T,L}$ and the differential dipole cross section $\frac{\mathrm{d}\sigma_{q\bar{q}}}{\mathrm{d}\vec{b}}$

- Scalar part of vector meson wave function
  - Gaus-LC
  - Boosted Gaussian

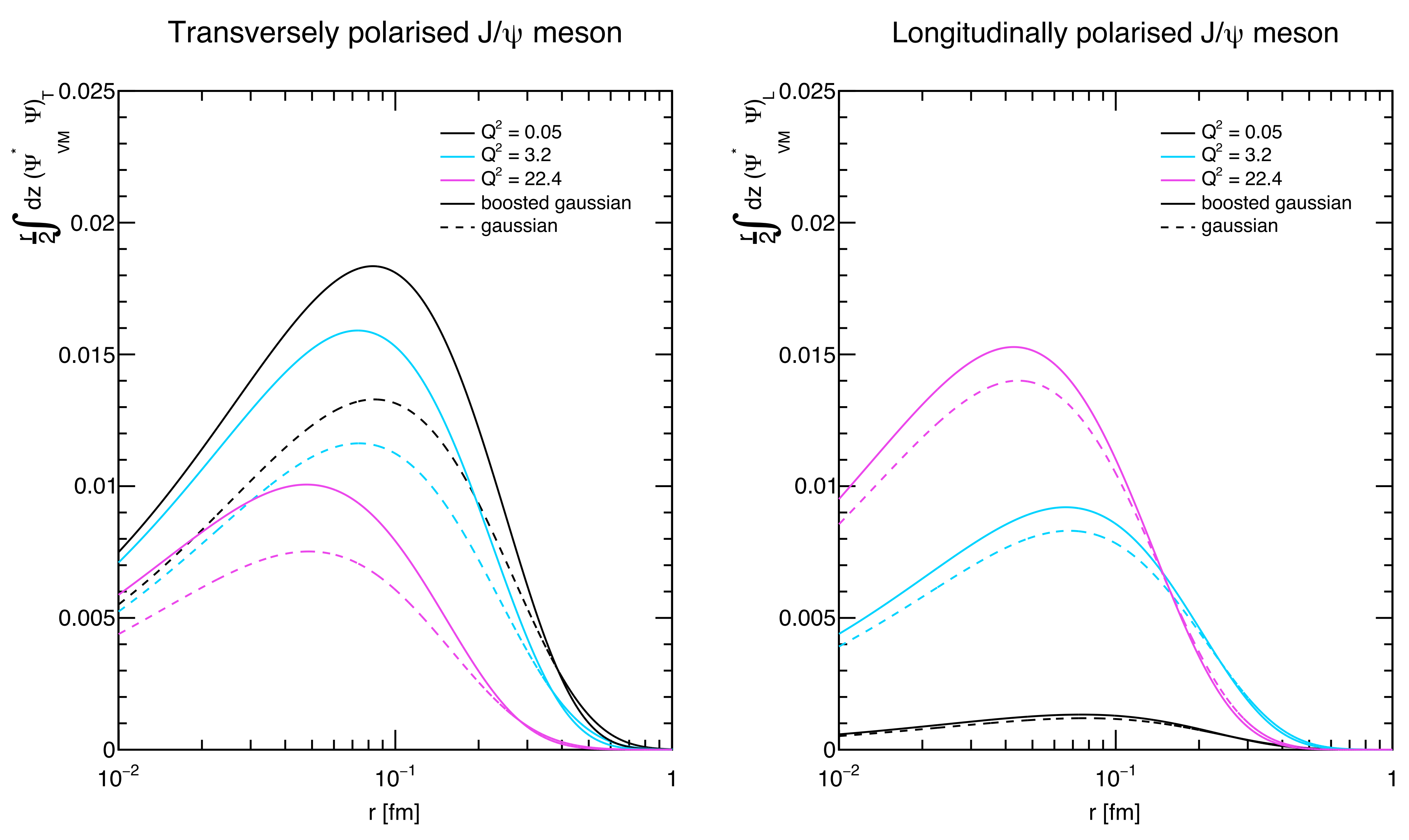

Vector meson production

- The differential dipole cross section

$$\frac{\mathrm{d}\sigma_{q\bar{q}}}{\mathrm{d}\vec{b}} = 2N(x,\vec{r},\vec{b}) \rightarrow \sigma_0 N(x,\vec{r}) T_p(\vec{b})$$

  - $\sigma_0 = 4\pi B_p$ is model dependent normalisation
  - Dipole amplitude $N(x,\vec{r}) \longrightarrow$ **GBW parameterisation:**

$$N(x,r) = 1 - \exp\left(-\frac{r^2 Q_s^2(x)}{4}\right), \text{ where } \quad Q_s^2(x) = Q_0^2\left(\frac{x_0}{x}\right)^{\lambda}$$

  - $T_p(\vec{b})$ describes the proton profile in transverse plane
    - **Gaussian distribution**
    - **Hot-spot model**

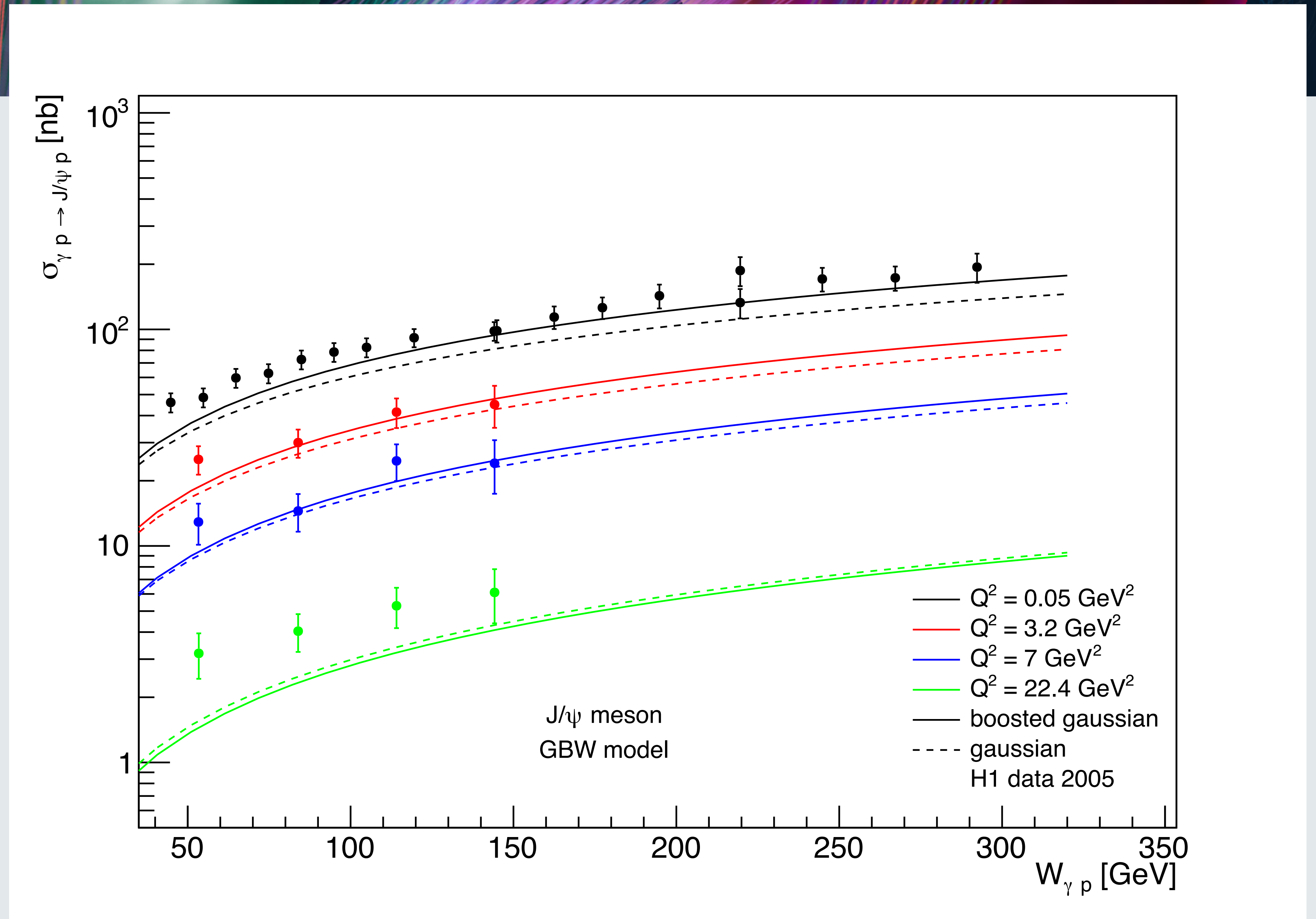

Total cross section of exclusive production of J/ψ meson using GBW parametrization.

Hot-spot model

- The transverse profile of the proton is seen as a set of localized regions of high partonic density - hot spots

$$T_p(\vec{b}) = \frac{1}{N_{hs}} \sum_{j=1}^{N_{hs}} T_{hs}(\vec{b} - \vec{b_j})$$

- Each hot spot follows a Gaussian distribution with the width B_{hs}, which can be interpreted as half of the average of the squared radius of the hot spot
- Position of hot spot is sampled from a two-dimensional Gaussian distribution centered at the origin $(0,0)$ with the width B_p

$$T_{hs}(\vec{b} - \vec{b_j}) = \frac{1}{2\pi B_{hs}} e^{-\frac{(\vec{b} - \vec{b_j})^2}{2B_{hs}}}$$

- The number of hot spots grows with energy and N_{hs} is generated integer value from a zero-truncated Poisson distribution with the mean value

$$\langle N_{hs}(x) \rangle = p_0 x^{p_1} \left(1 + p_2 \sqrt{x}\right)$$

  - p_0, p_1, p_2 are free parameters, whose value depend on energy dependance of B_p and B_{hs}

Hot-spot model

- Quantities $B_p = 4.7\,\mathrm{GeV}^{-2}$ and $B_{hs} = 0.8\,\mathrm{GeV}^{-2}$ are fixed.
- Based on measurements from HERA, it is possible to assume that the radius of the proton $B_p(W)$ has logarithmic growth with energy

$$B_p(W) = 4.63 + 4\alpha' \ln\left(\frac{W}{90}\right), \quad \text{where} \quad \alpha' = 0.164\,\mathrm{GeV}^{-2} \quad \text{(photoproduction)}$$

- It is also possible to consider that B_{hs} is inversely related to the saturation scale, which implies a shrinking size of hot spots as the saturation scale increases

$$B_{hs}(x) = k\frac{1}{Q_s^2}, \quad \text{where} \quad k = \frac{1}{2}$$

- Change in size of the proton and sizes of hot spots, necessitates corresponding modification in N_{hs}, which is achieved by modifying the parameters p_0, p_1 and p_2

- The amplitude is calculated using $10\,000$ configurations of the proton profile function for each value of x
  - Exclusive cross section → average over geometrical configurations
  - Dissociative cross section → variance over geometrical configurations

Shape of the transverse profile of the proton

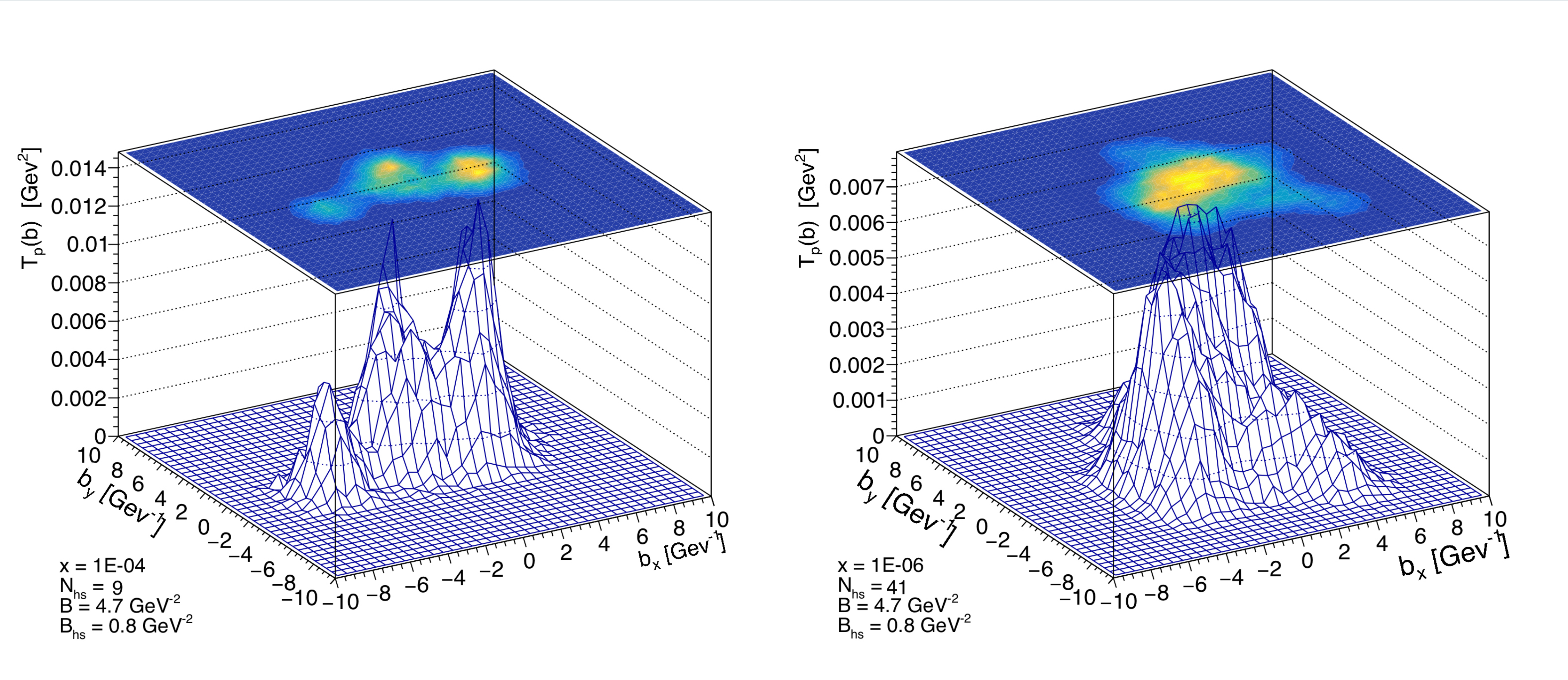

fixed B_p and B_{hs} for different values of x

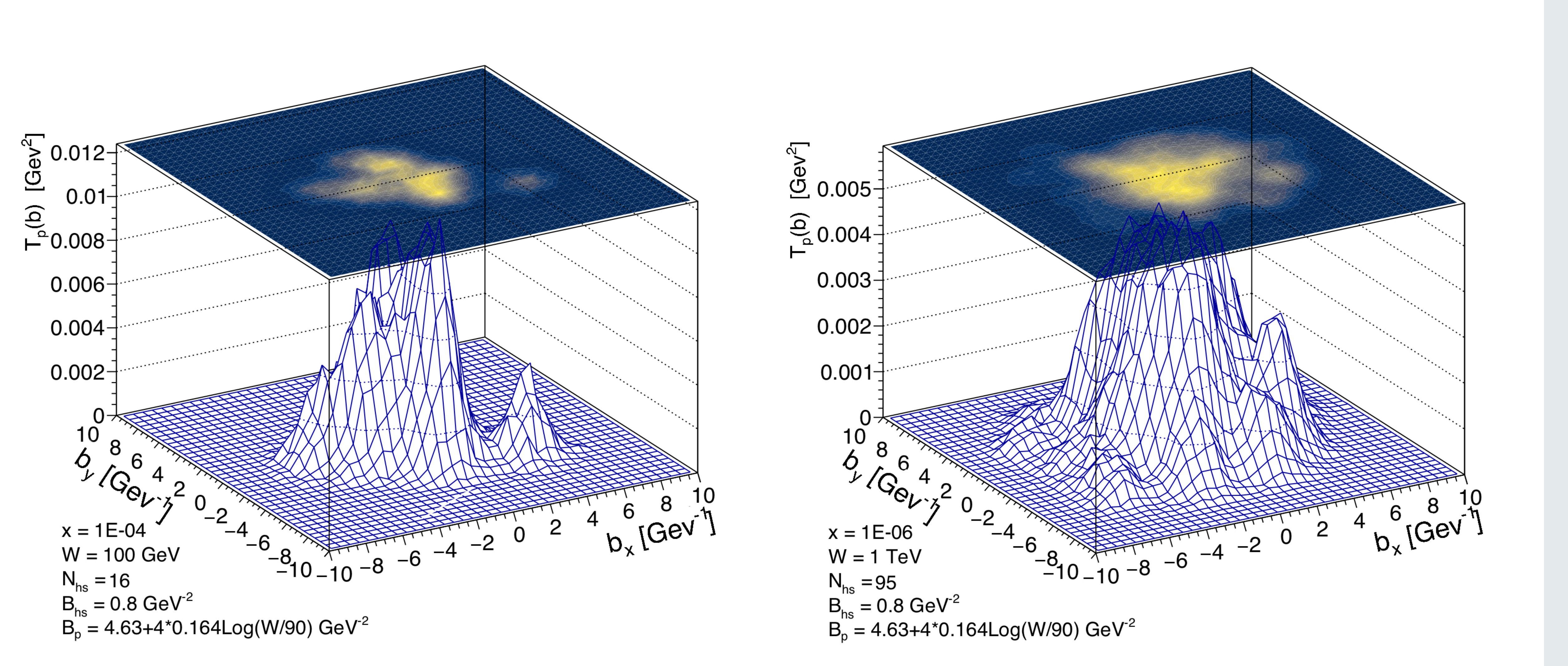

energy dependent $B_p(W)$ and fixed value of B_{hs}

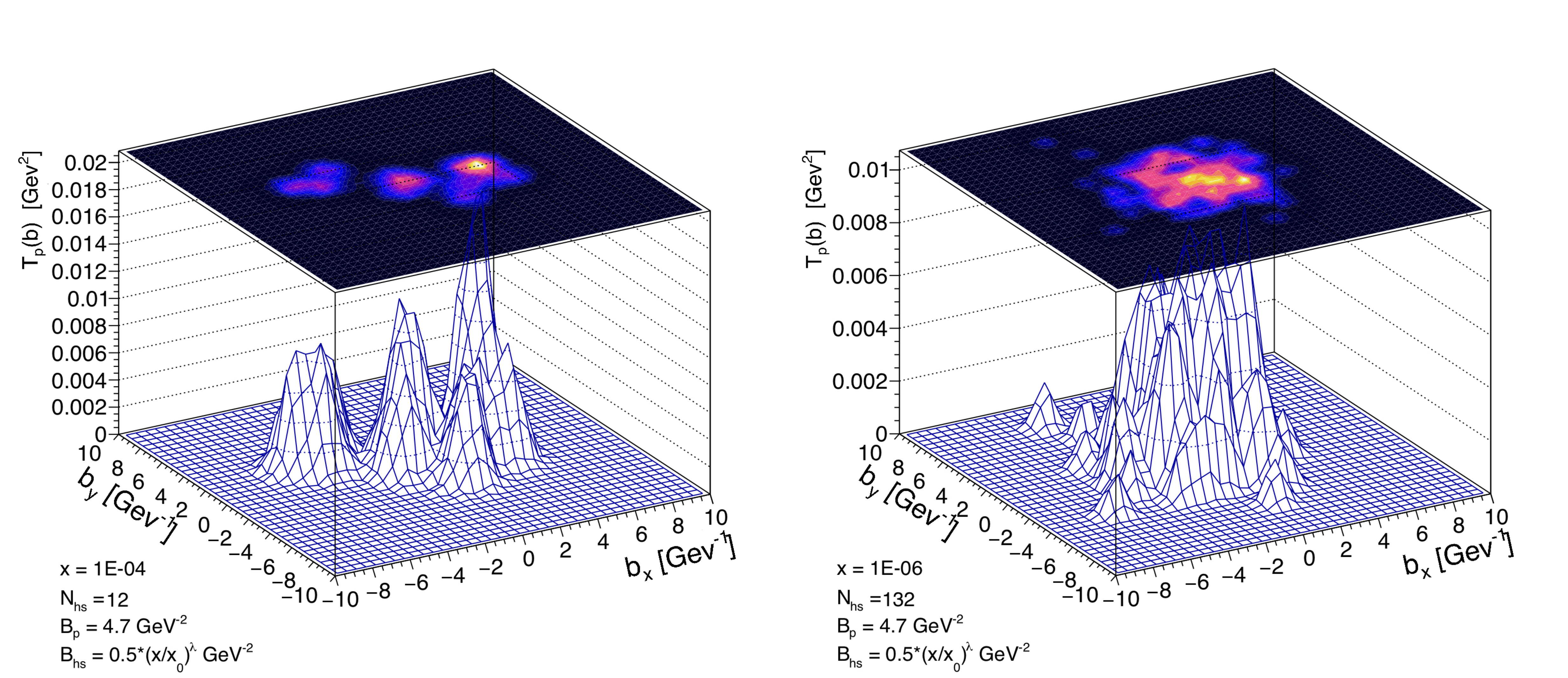

fixed value of B_p and energy dependent $B_{hs}(x)$

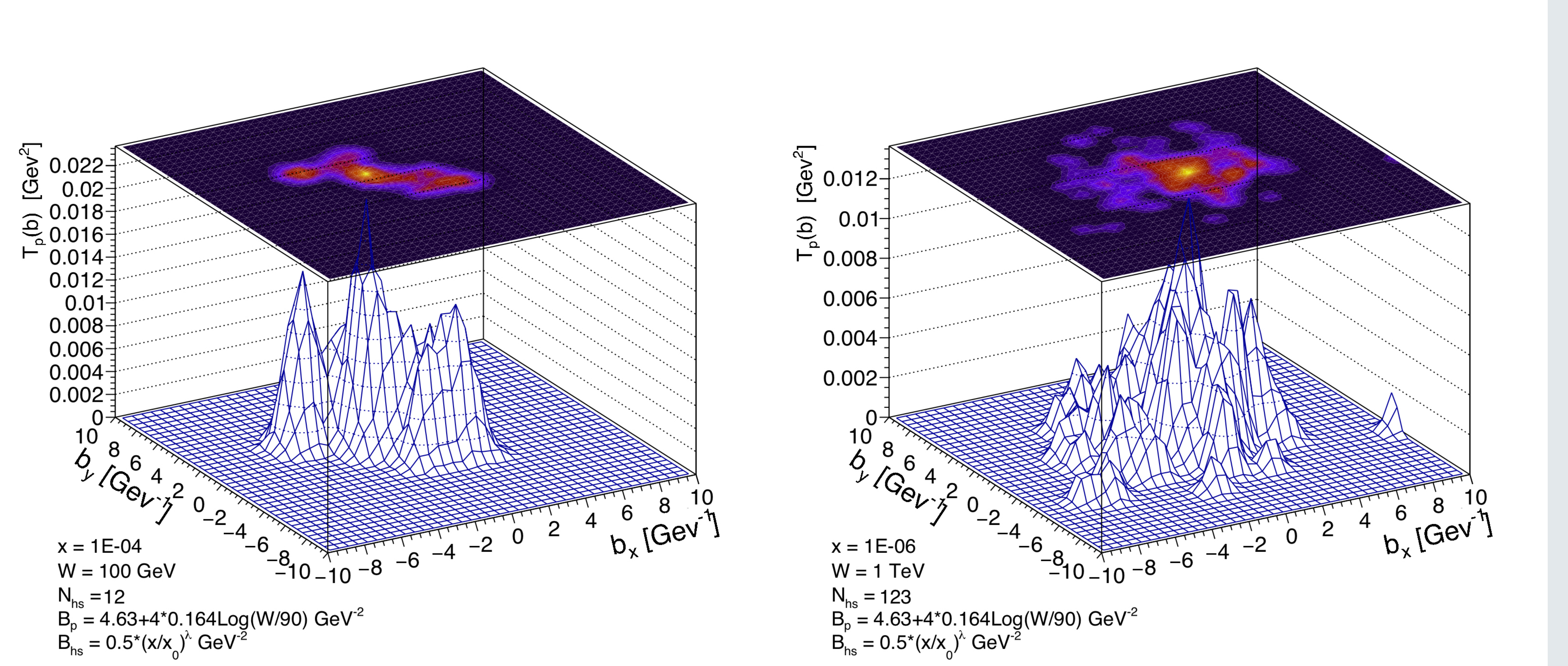

energy dependent $B_p(W)$ and $B_{hs}(x)$

Fixed B_p and B_{hs}

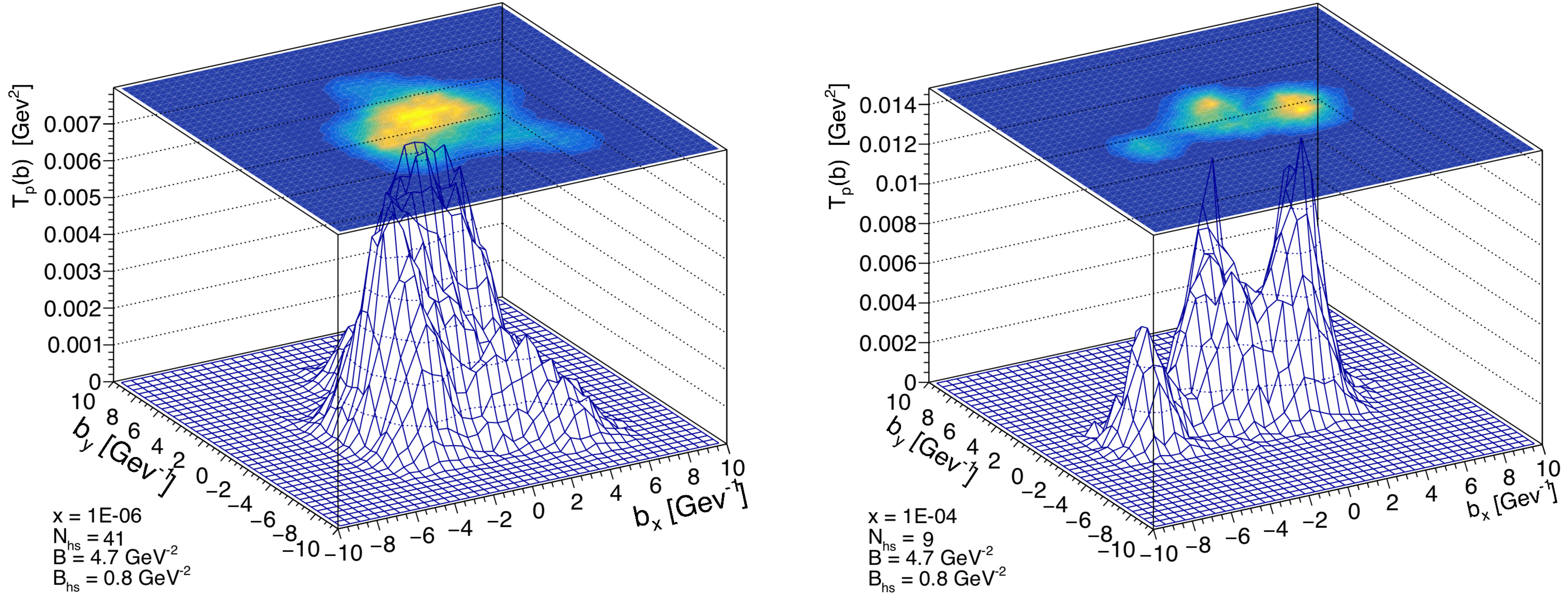

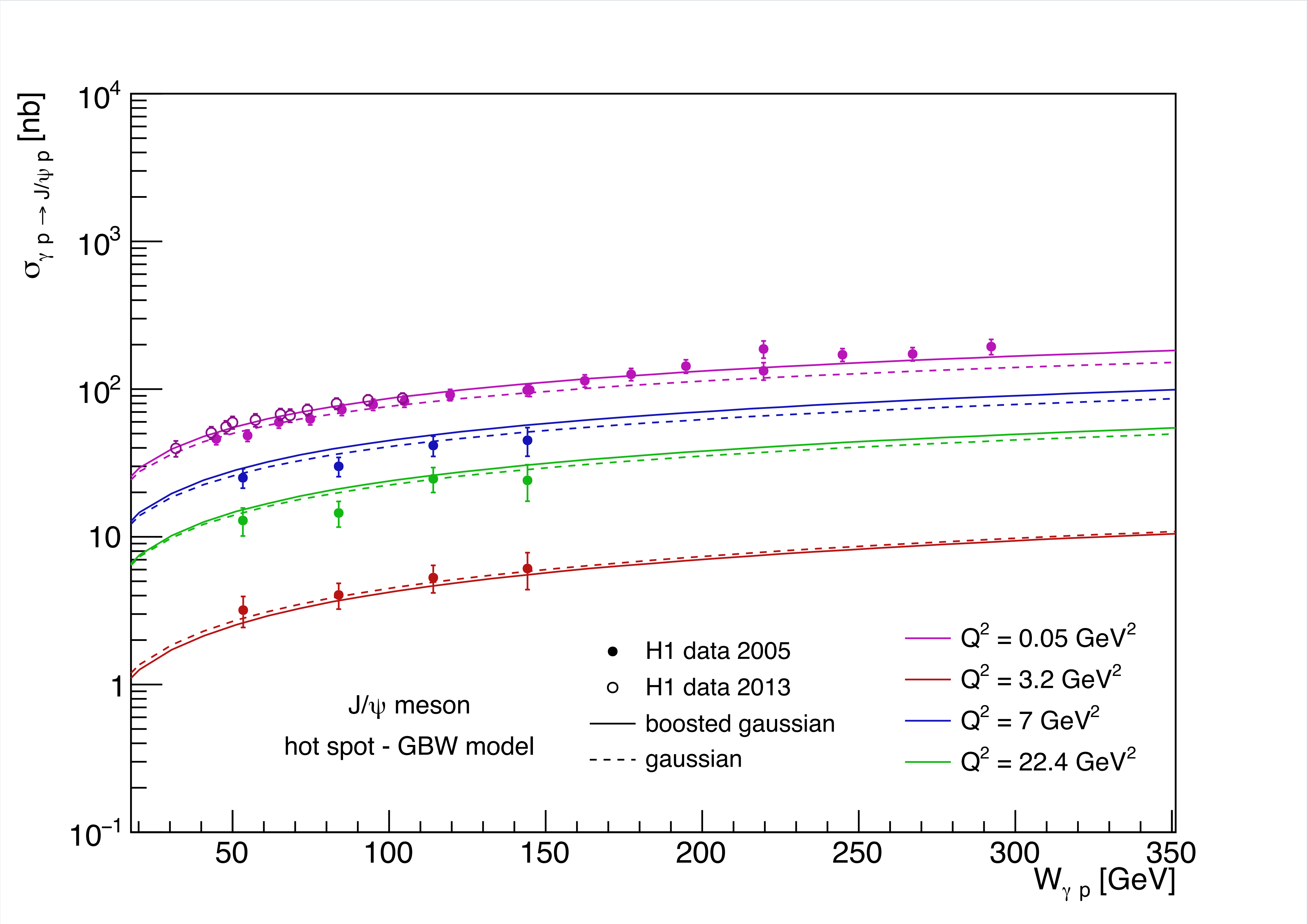

total cross section of exclusive J/ψ production

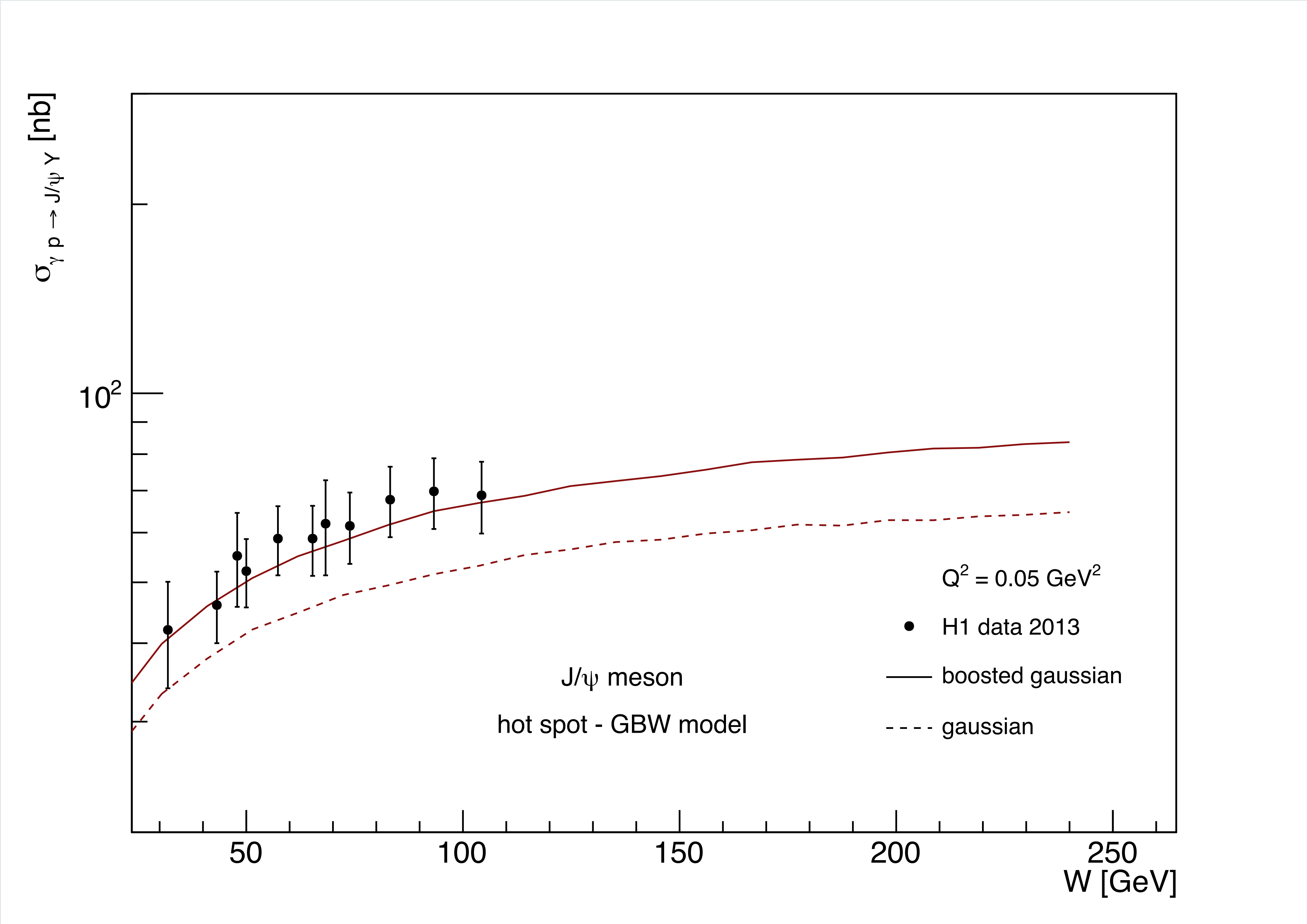

total cross section of dissociative J/ψ production

- The results for the total cross section of exclusive and dissociative production of the J/ψ vector mesons as functions of W, compared with measurements from H1

Energy-dependent $B_p(W)$ and fixed B_{hs}

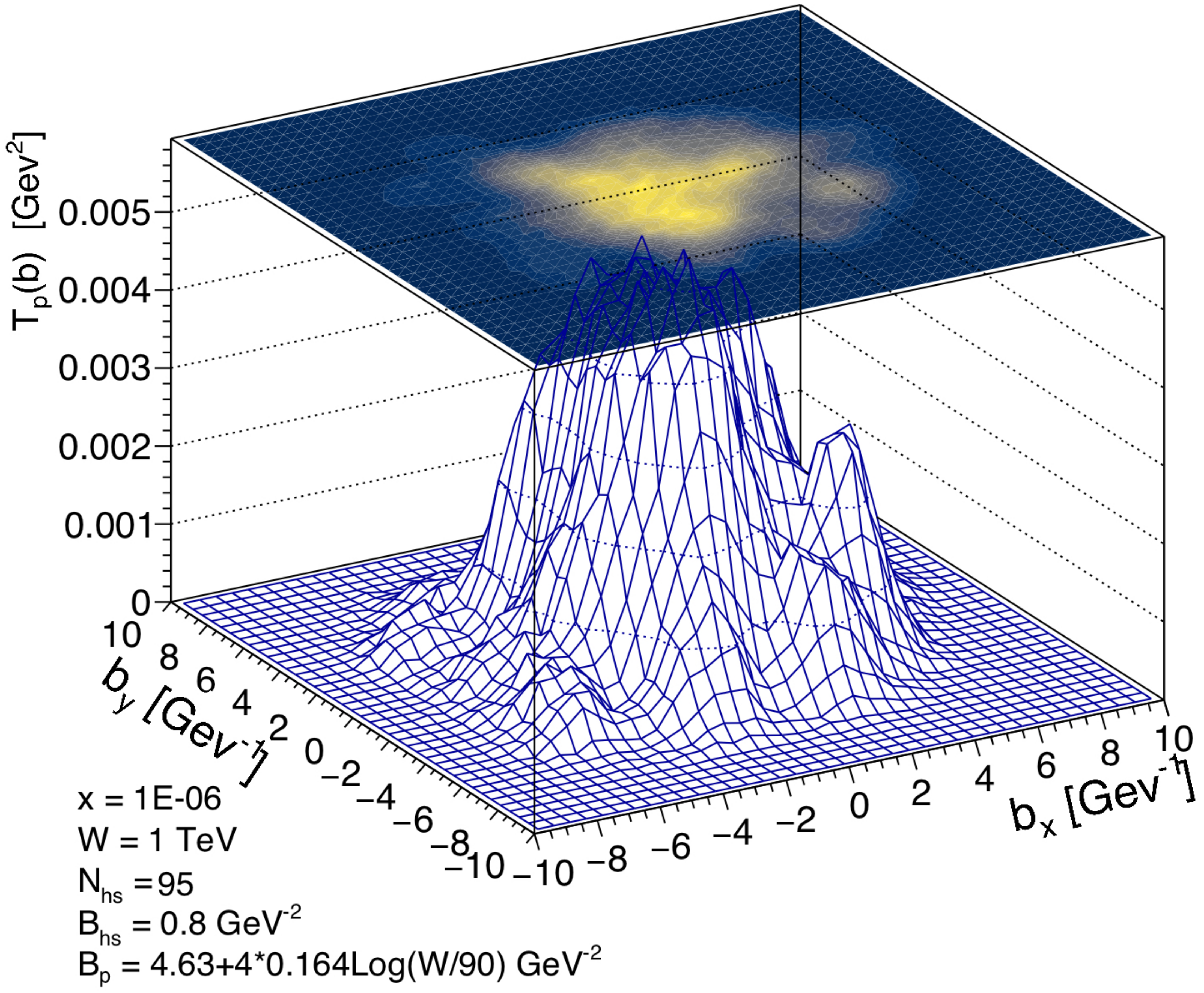

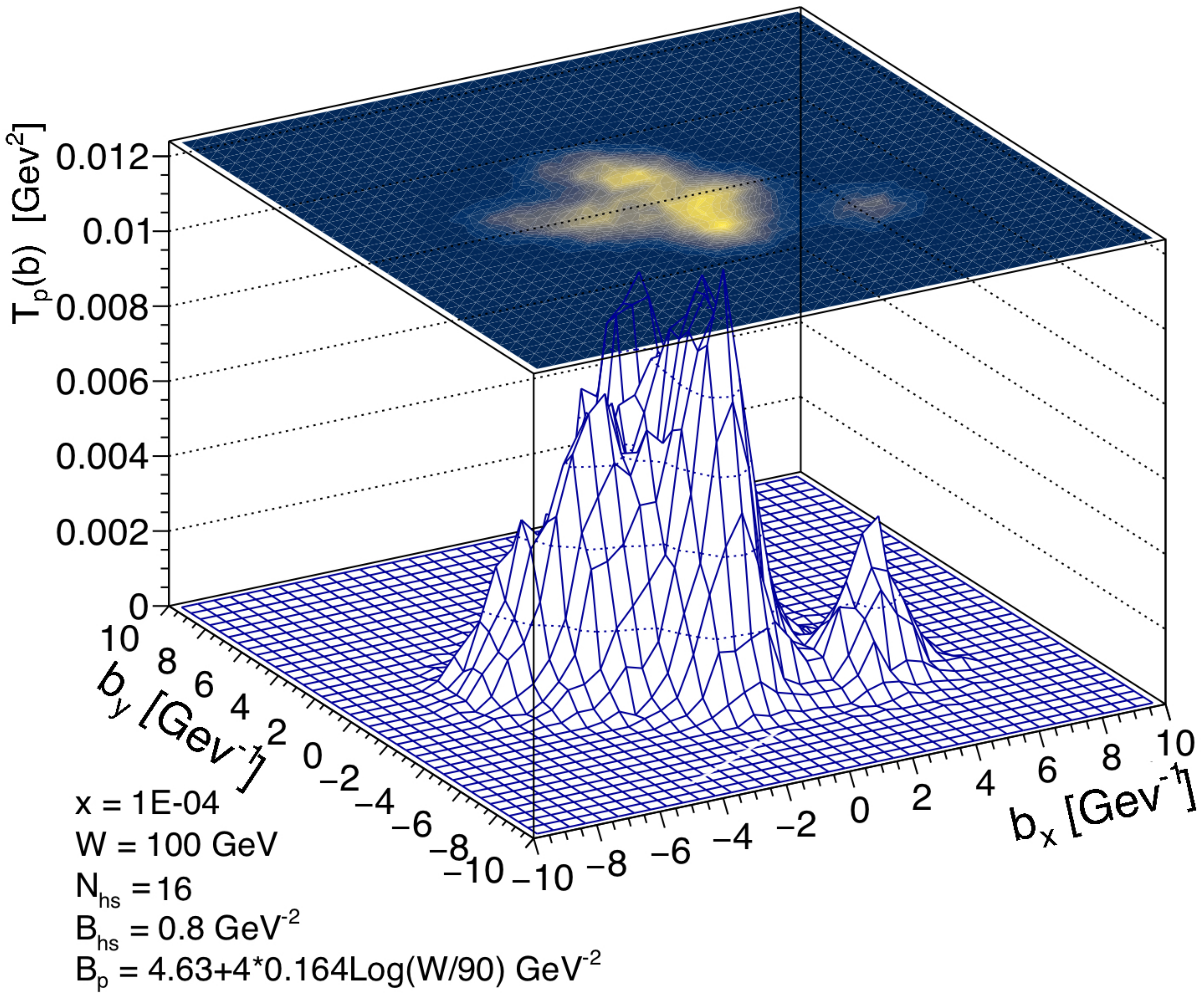

- Comparison of the model predictions for the total cross section of exclusive J/ψ photoproduction using fixed B_p (black line) and energy-dependent $B_p(W)$ (blue line) with H1 and ALICE data
- The energy-dependent $B_p(W)$ follows a logarithmic scaling with respect to W, indicating the growth of the proton size with energy → modification of p_0, p_1 and p_2 in N_{hs}

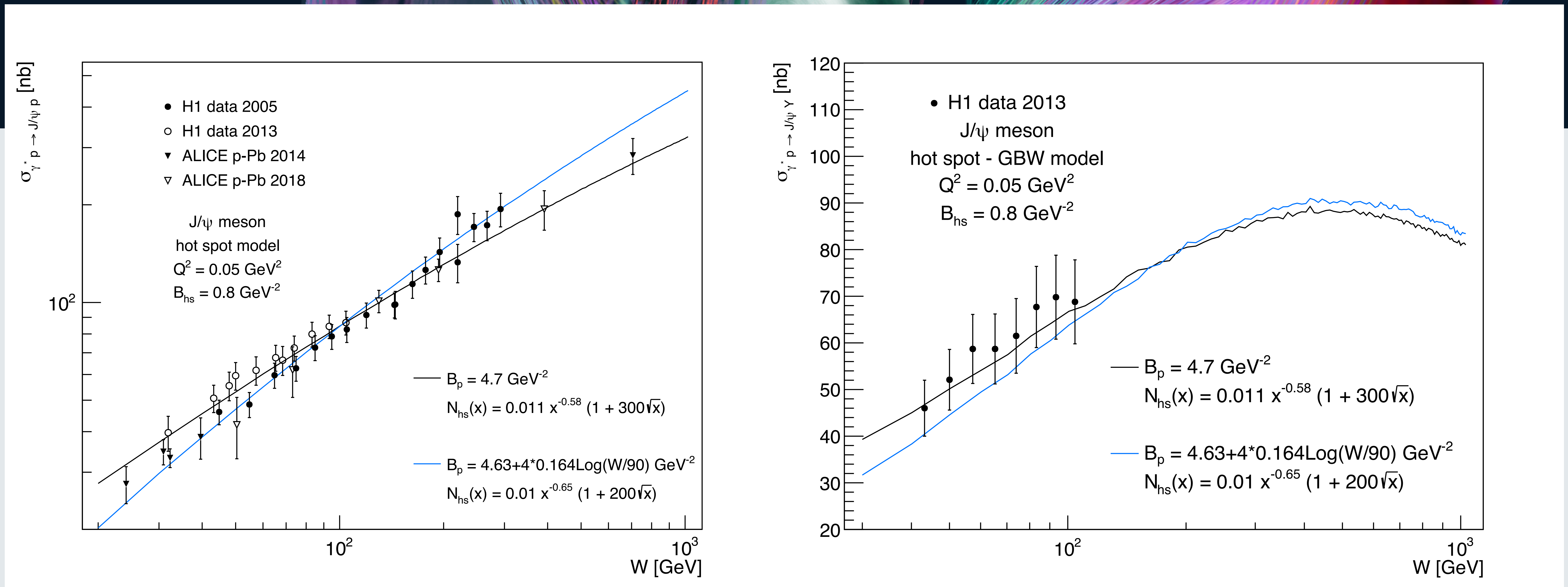

total cross section of exclusive and dissociative J/ψ photoproduction using fixed B_p and energy-dependent $B_p(W)$

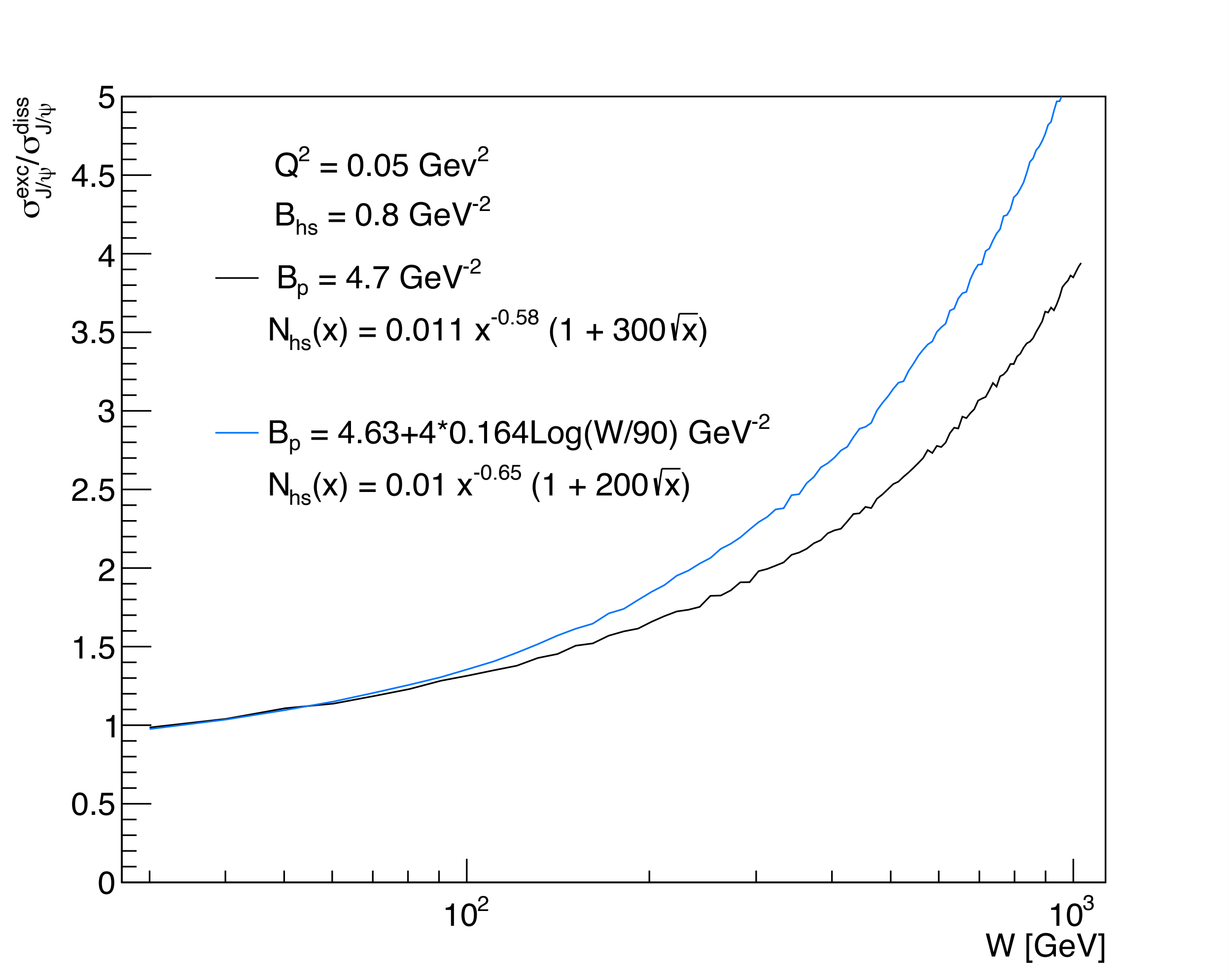

Ratio of the exclusive and dissociative cross section

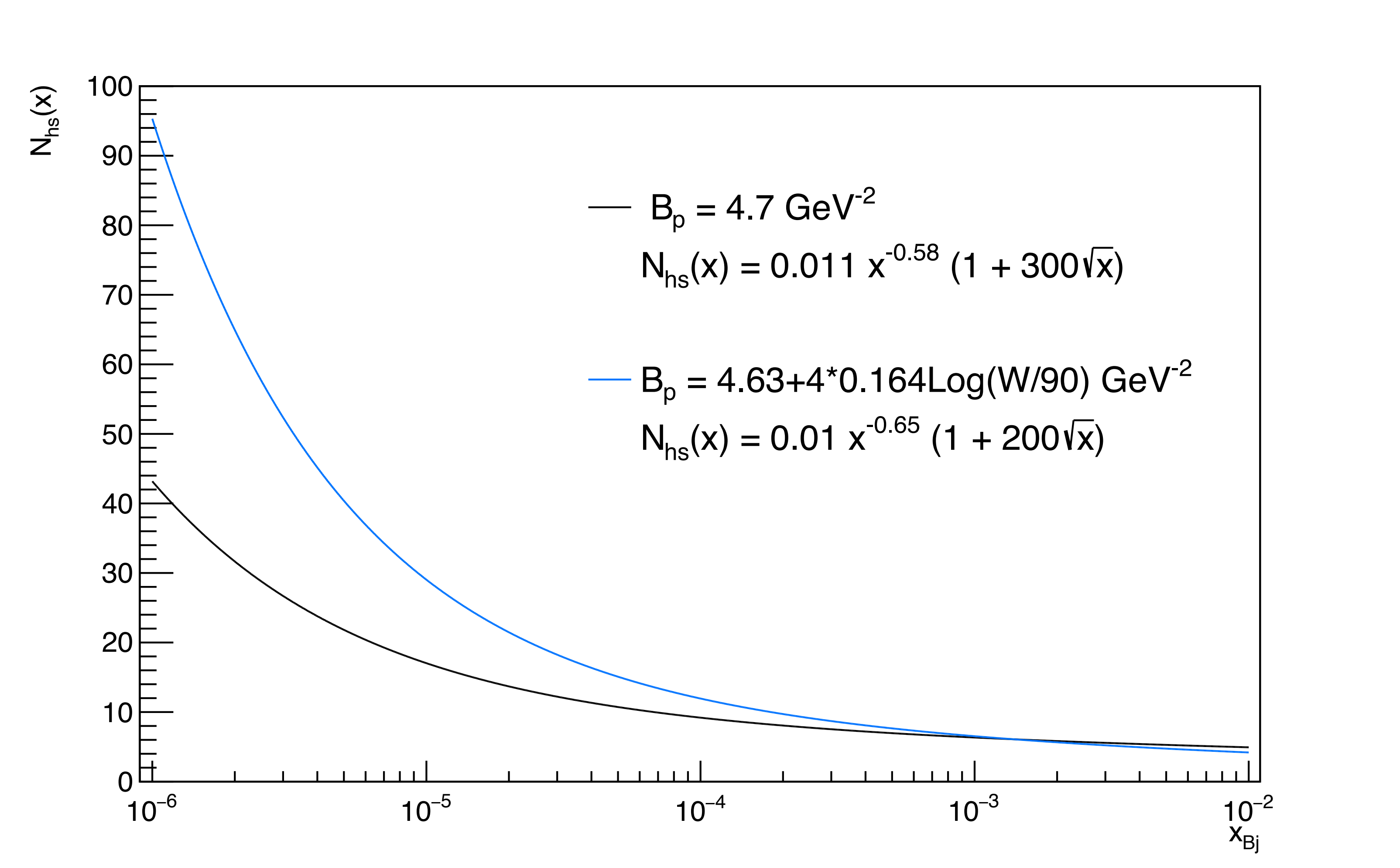

Number of hot spots for energy-dependent and energy-independent slope parameter

Fixed B_p and energy-dependent $B_{hs}(x)$

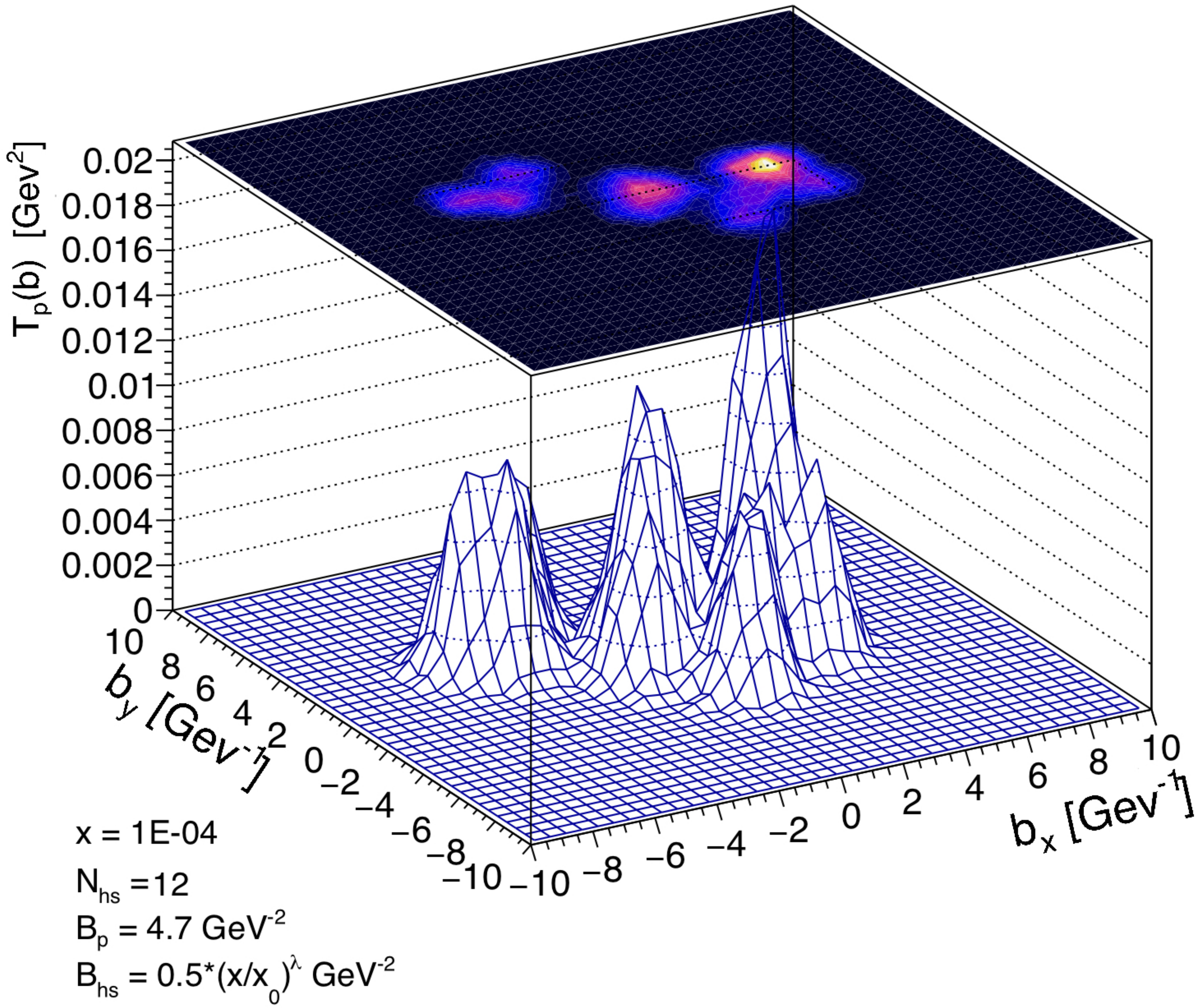

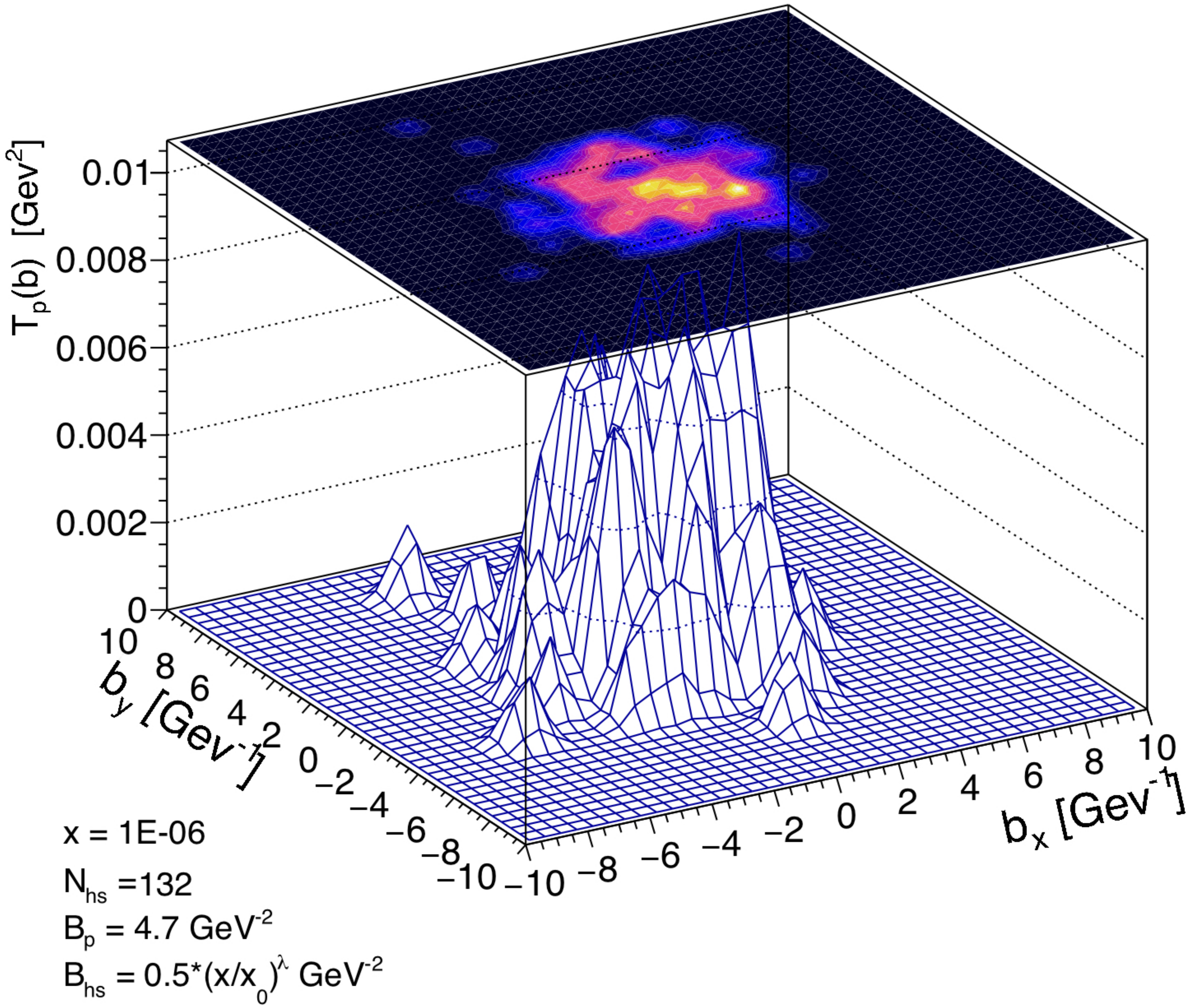

- Comparison of the model predictions for the total cross section of exclusive J/ψ photoproduction using fixed B_{hs} (black line) and energy-dependent $B_{hs}(x)$ (red line) with H1 and ALICE data
- At higher energies, smaller hot spots will emerge → adjustment in N_{hs}

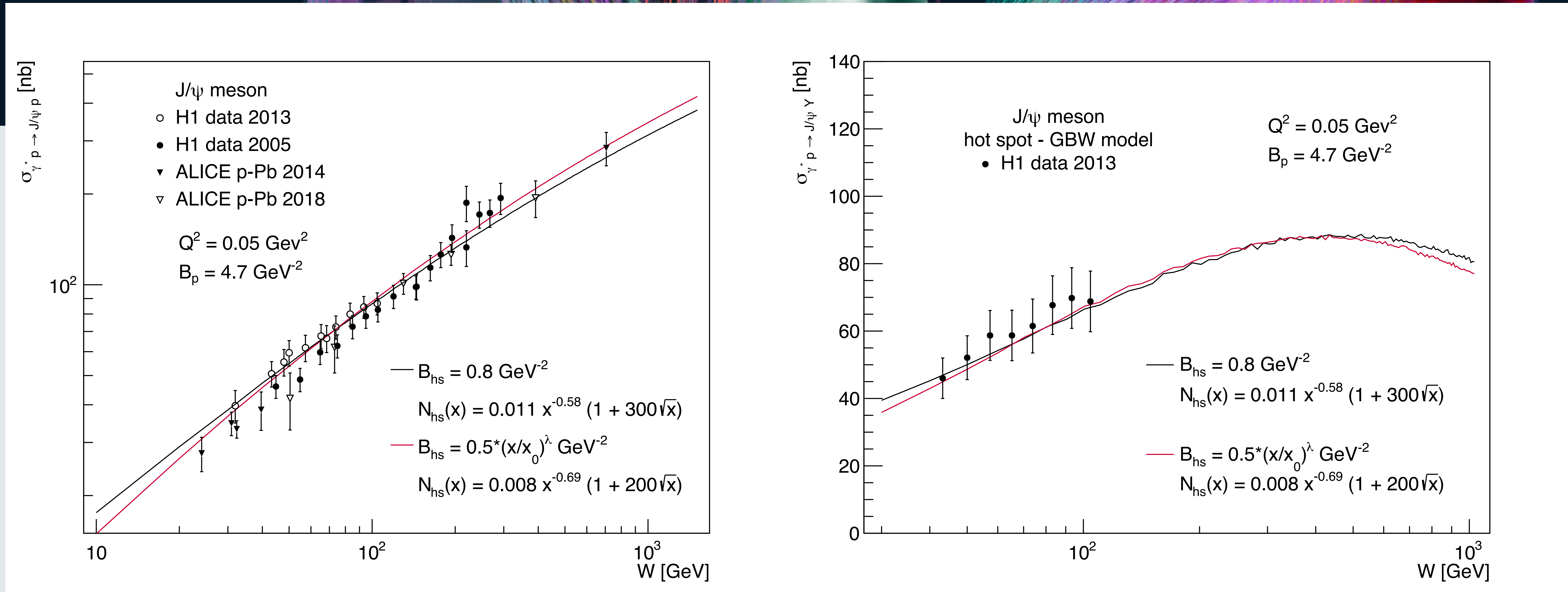

total cross section of exclusive and dissociative J/ψ photoproduction using fixed B_{hs} and energy-dependent $B_{hs}(x)$

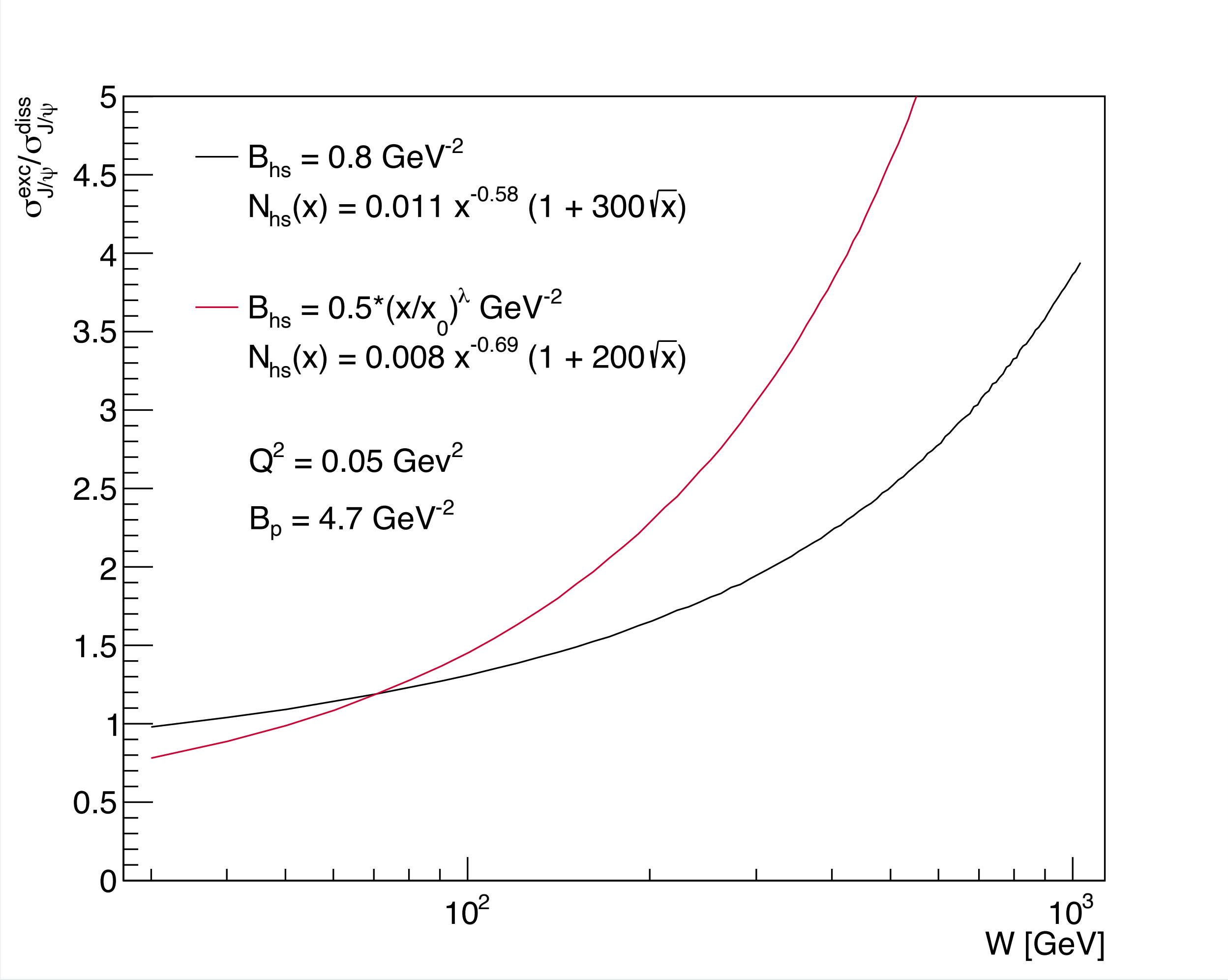

Ratio of the exclusive and dissociative cross section

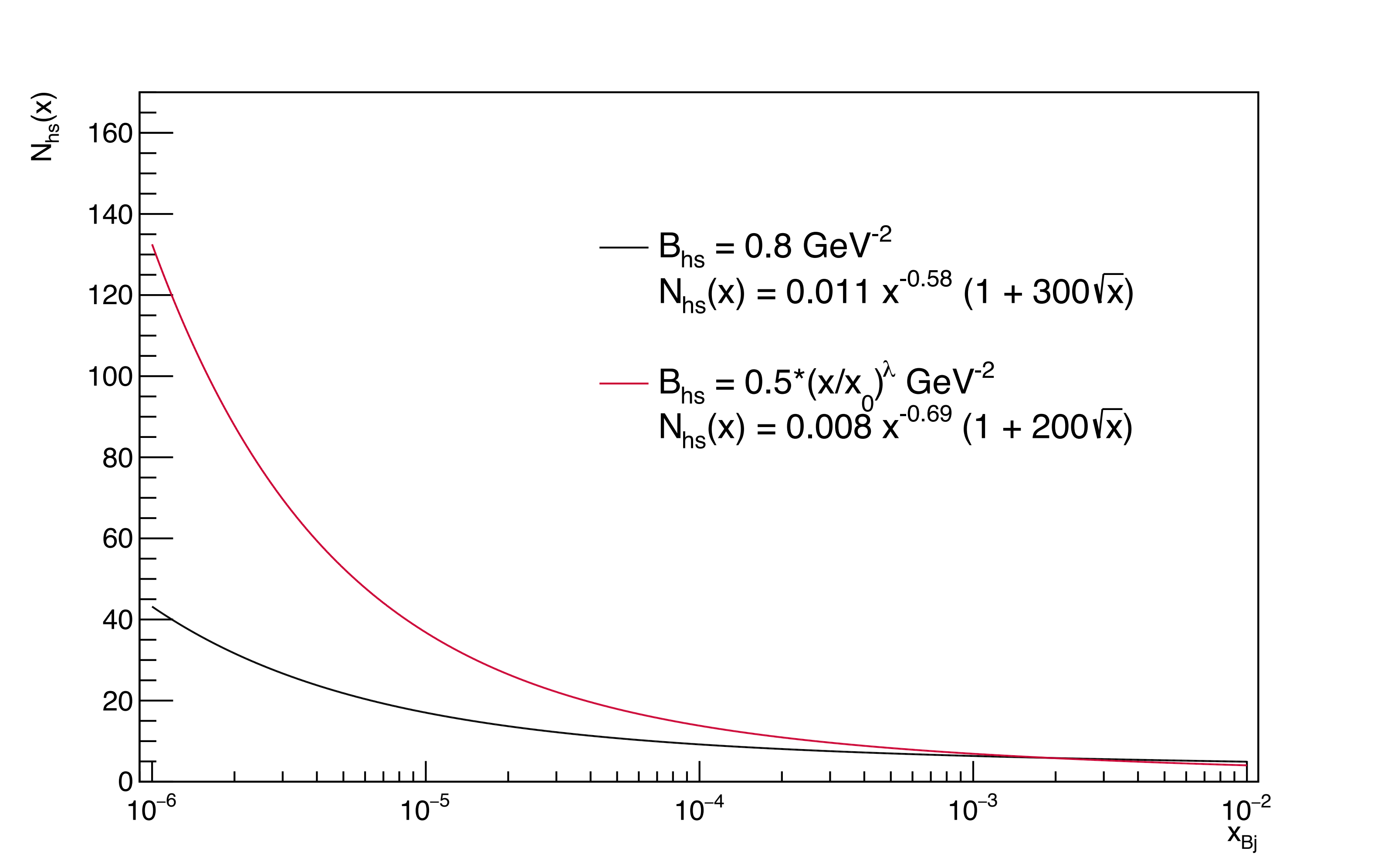

Number of hot spots for energy-dependent and energy-independent hot spot radius

Energy dependent $B_p(W)$ and $B_{hs}(x)$

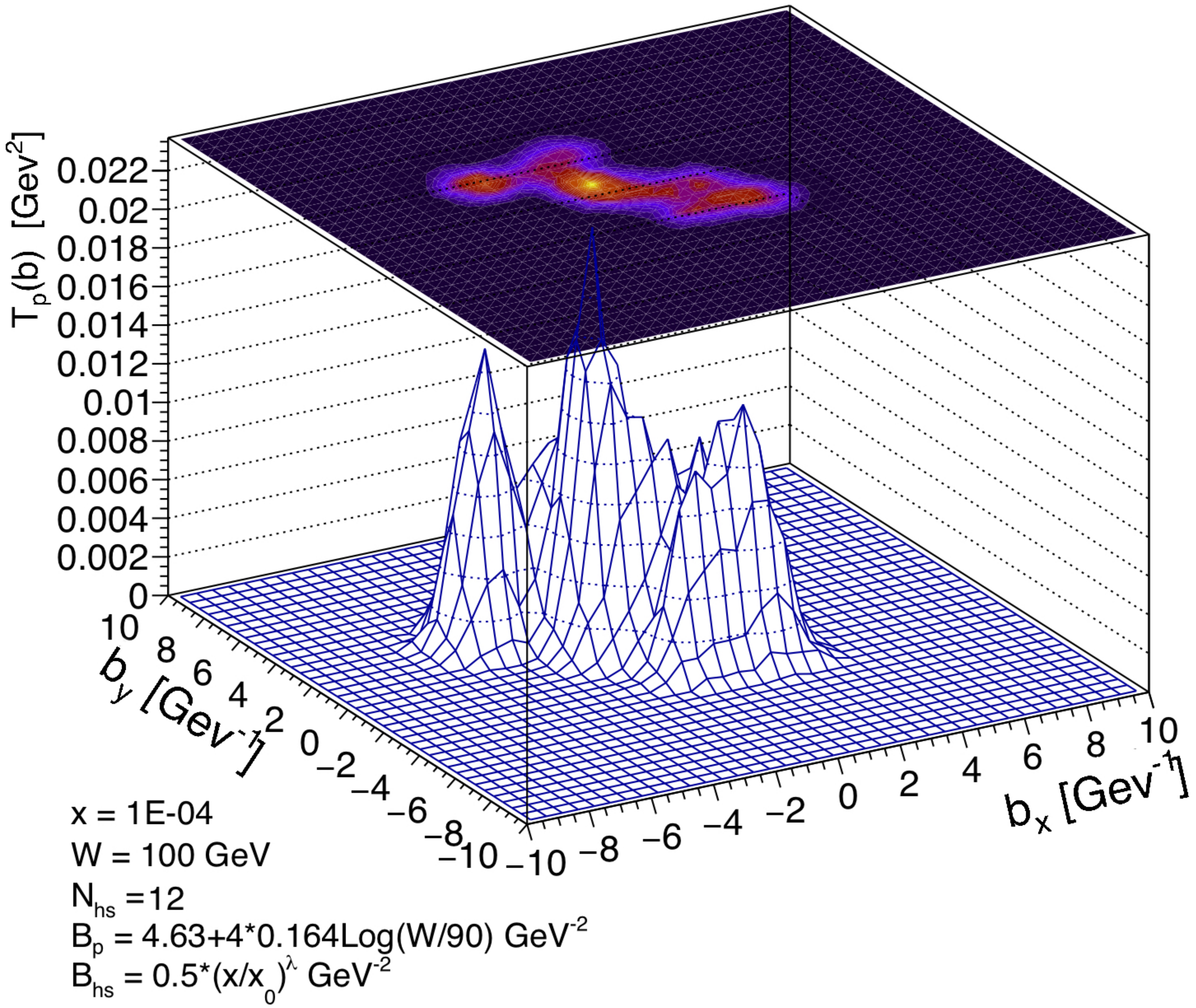

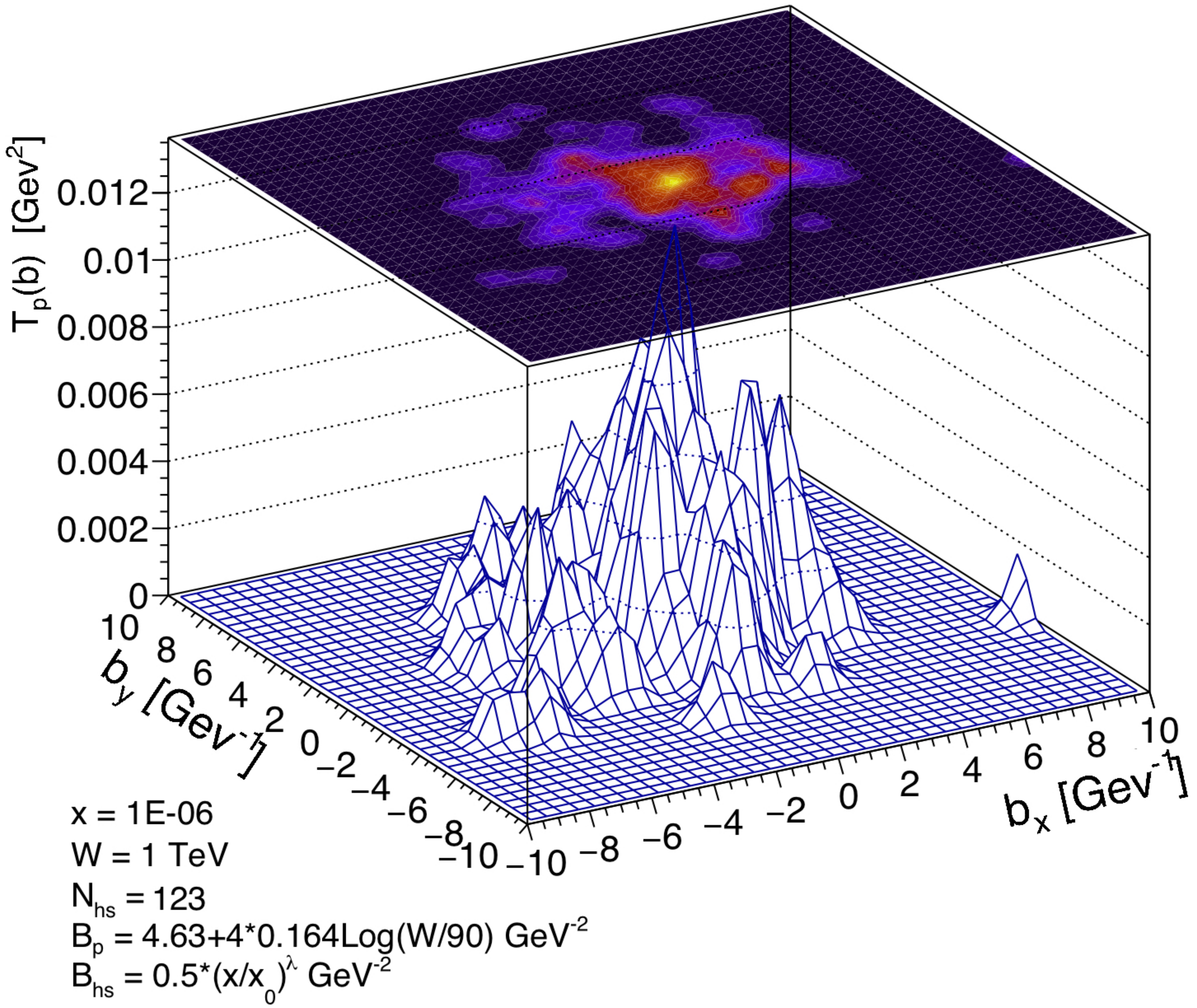

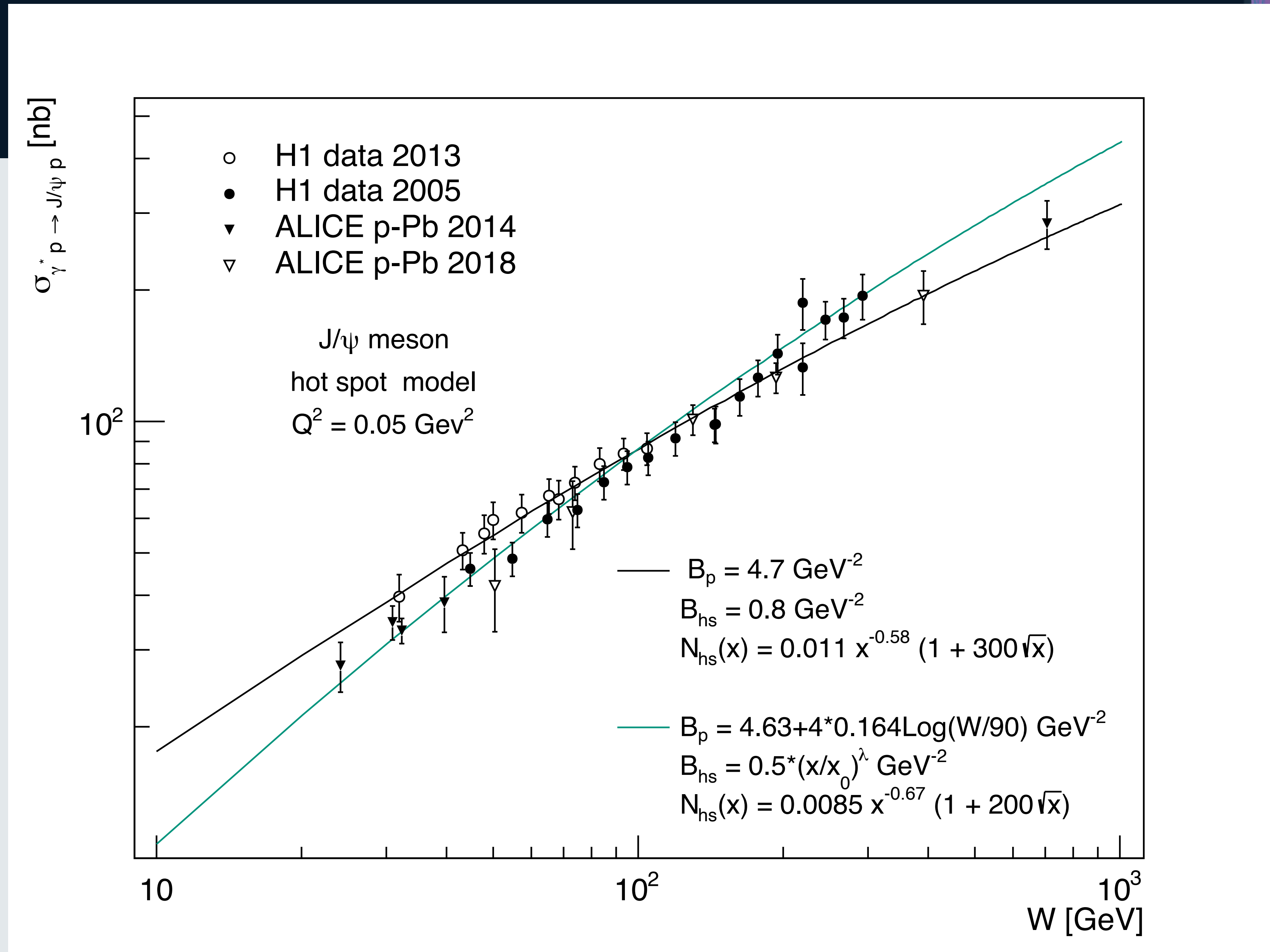

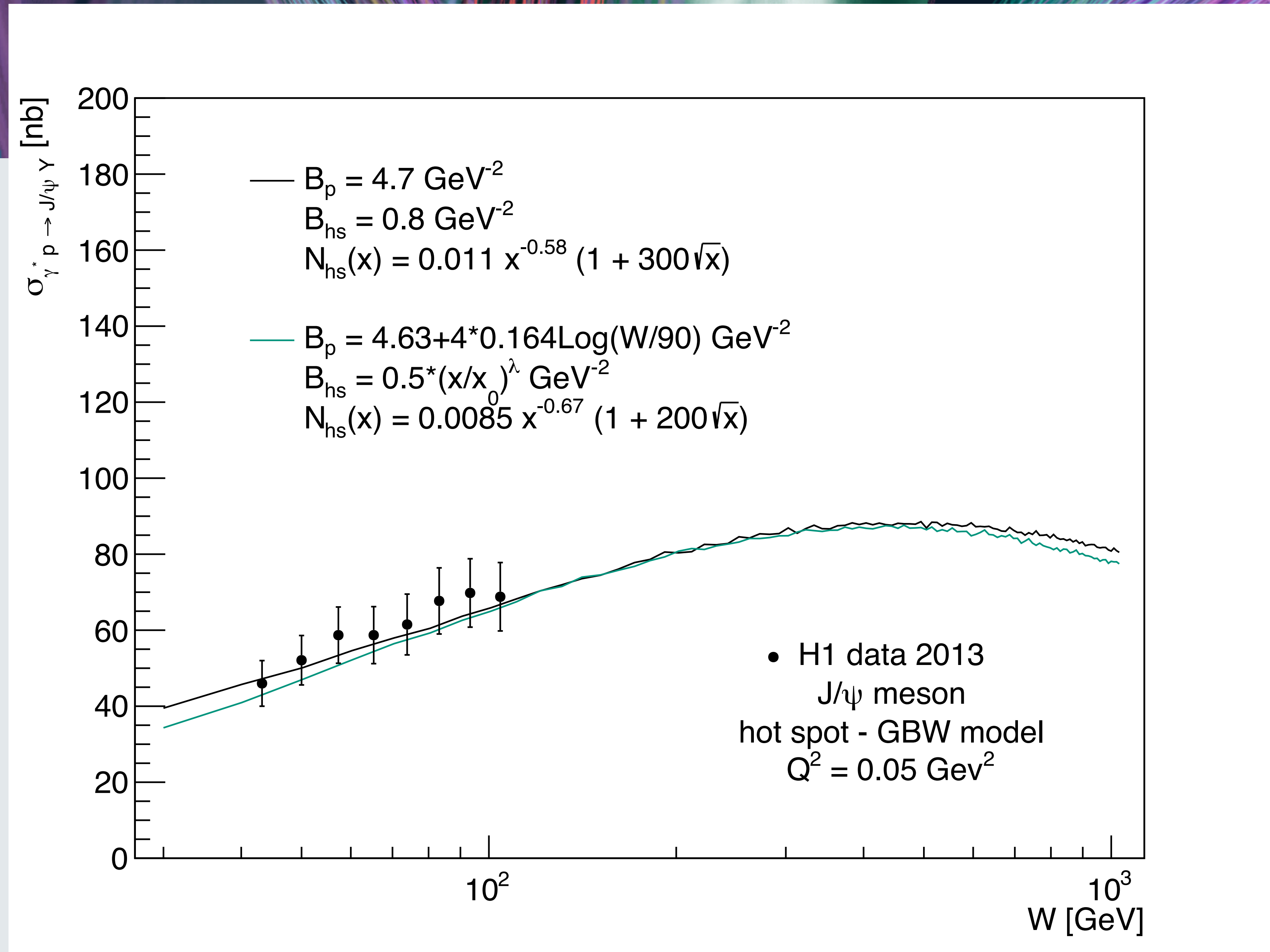

total cross section of exclusive and dissociative *J/ψ* photoproduction using energy-dependent and energy-independent B_p and B_{hs}

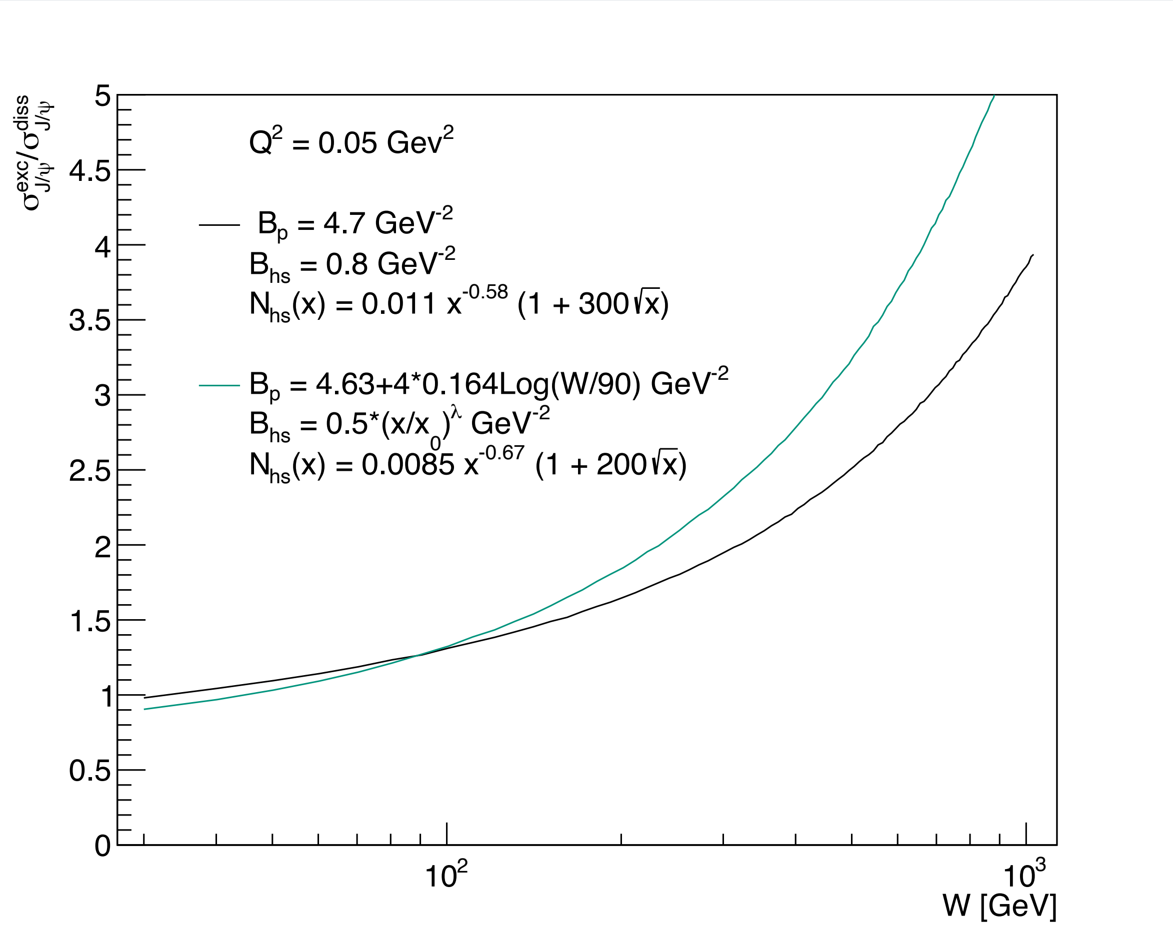

Ratio of the exclusive and dissociative cross section

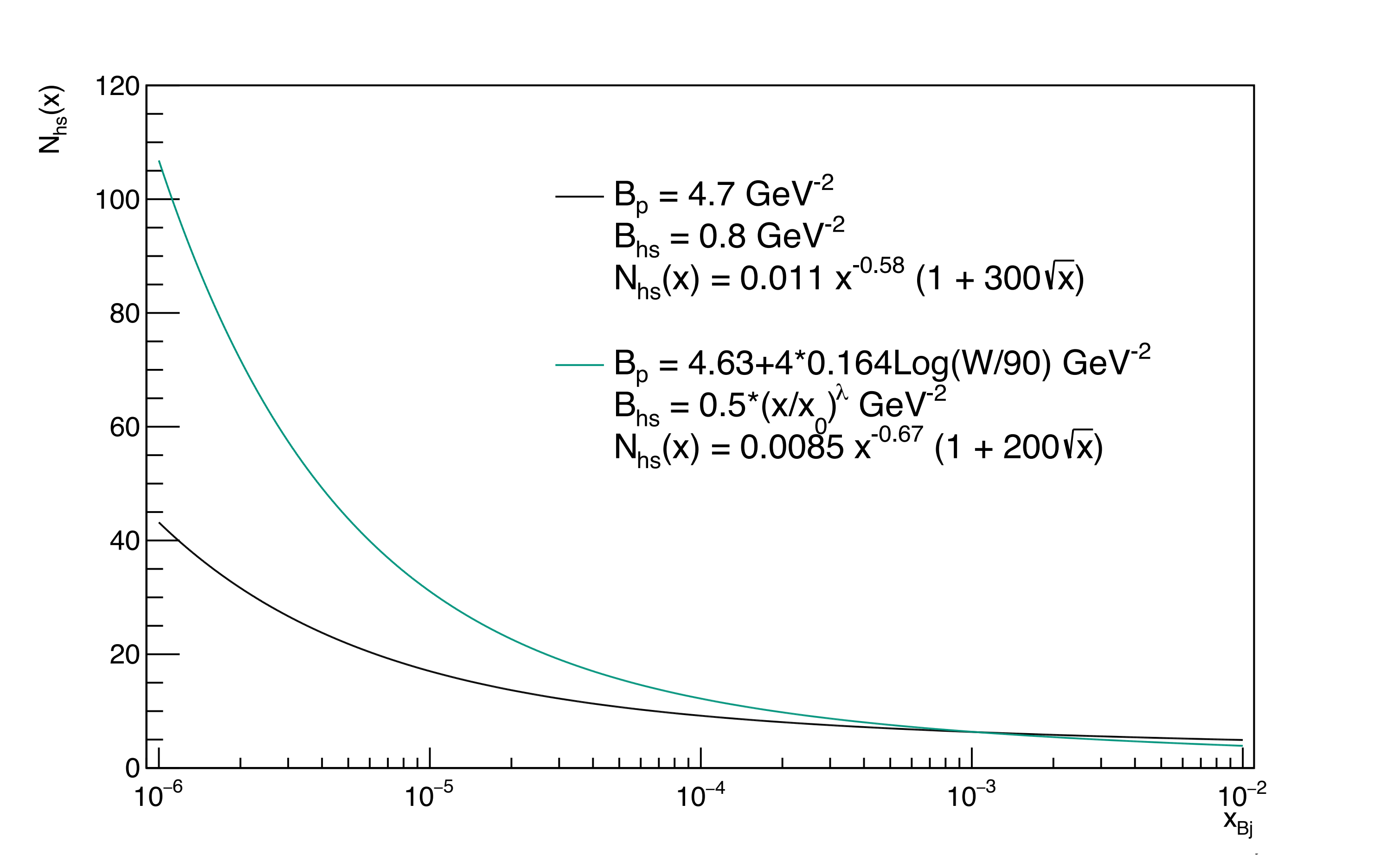

Number of hot spots for energy-dependent and energy-independent B_p and B_{hs}

Summary

- GBW model for the dipole cross section

  → Gaussian distribution and Hot-spot model were used to describe the proton profile in transverse plane

- Four different Hot-spot model scenarios based on the energy dependence of the size of the proton and sizes of hot spots were used

  → logarithmic growth of radius of the proton with energy

  → shrinking size of hot spots with increasing saturation scale

    → correlation between energy dependent parameter and the number of hot spots

    → these models generally demonstrate a steeper evolution of the total cross section of exclusive J/ψ production compared to models with fixed Bp and Bhs.